Chapter 25
Measuring Soil Erosion Rates Using Natural (^{7}Be, ^{210}Pb) and Anthropogenic (^{137}Cs, ^{239,240}Pu) Radionuclides

Gerald Matisoff and Peter J. Whiting

Abstract This chapter examines the application of natural (^{7}Be and ^{210}Pb) and anthropogenic fallout radionuclides (^{134}Cs, ^{137}Cs, ^{239,240}Pu) to determine soil erosion rates. Particular attention is given to ^{137}Cs because it has been most widely used in geomorphic studies of wind and water erosion. The chapter is organized to cover the formation and sources of these radionuclides; how they are distributed in precipitation and around the globe: their fate and transport in undisturbed and tilled soils; and their time scales of utility. Also discussed are methods for soil collection, sample preparation for ^{137}Cs analysis by gamma spectroscopy, and the selection of standards and instrument calibration. Details are presented on methods for calculating soil erosion, including empirical methods that are related to the Universal Soil Loss Equation (USLE), box models that compare ^{137}Cs activities in a study site to a reference site, and time dependent methods that account for the temporal inputs of ^{137}Cs and precipitation induced erosion. Several examples of recent applications, including the combination of radionuclides with other techniques or measurements, are presented. The chapter concludes with suggestions for future work: the value of new methods and instrumentation to allow for greater spatial resolution of rates and/or greater accuracy; the need to incorporate migration of radionuclides in the time-dependent models; the opportunities to concurrently use the global and Chernobyl signals to better understand temporal variation soil erosion processes and rates; and the importance of the use of these tracers to characterize C storage and cycling.

G. Matisoff (✉) and P.J. Whiting
Department of Geological Sciences, Case Western Reserve University, Cleveland, OH 44106-7216, USA
e-mail: gerald.matisoff@case.edu; peter.whiting@case.edu

25.1 Introduction

25.1.1 Soil Erosion; Nature of the Problem

Soil is among our most fundamental resources and soil processes help regulate atmospheric composition and climate. Soil anchors and sustains the vegetation that provides sustenance for animals and humans and provides fibers and material used in everything from cotton for clothing to lumber for homes to biomass for energy. The soil itself can be mined for key materials, minerals and metals, and energy. The foundations of most human structures – homes, buildings, and roads – are built on soil. Soil and soil processes filter water, reduce toxicity of airborne pollutants delivered to the land surface, and store carbon and nutrients. The value of soil in terms of ecosystem function and service has been estimated in the hundreds of billions of dollars per year (Pimental et al. 1995).

A comprehensive understanding of material fluxes on the earth surface and its effects on geochemical cycles (hydrologic, C, and N), atmospheric composition and climate, and ocean chemistry depends upon an understanding of soil and soil movement on the landscape including erosion, transport, and deposition. Soils sequester C and N from the atmosphere and retain certain metals during the weathering of rocks, but soil erosion either moves those materials to places of long-term storage or exposes soils to greater reactivity. Soils hold 2,300 Gt of carbon, about four times as much carbon as is in the atmosphere (Lal 2003). It has been suggested that if carbon on the landscape lost by erosion is replaced by new vegetative growth, then intermediate storage in fluvial systems of the eroded carbon represents a net removal of carbon from the atmosphere and

M. Baskaran (ed.), *Handbook of Environmental Isotope Geochemistry*, Advances in Isotope Geochemistry,
DOI 10.1007/978-3-642-10637-8_25,

may be the "missing" anthropogenic carbon (Harden et al. 1992; Stallard 1998). Others note that oxidation of a portion of the carbon in transport may produce 0.8–1.2 GtC per year. Thus anthropogenically enhanced soil erosion may reinforce global warming.

Soil is moved by a variety of processes including water (splash, sheetwash, rills), wind, ice (freeze-thaw, glaciers, periglacial), gravity (dry ravel, creep, toppling, debris flows, earthflows), tillage, and bioturbation. Erosion is often accelerated by disturbance (clearing, fire, plowing, overgrazing, compaction, or desiccation) that disrupts soil structure and removes vegetative covering. Oldeman (1994) estimated that 1,094 Mha (1 ha = 10^4 m^2) are affected by water erosion and 549 Mha by wind erosion. These numbers represent 12 and 6% of agricultural land areas, respectively. Total erosion of these areas is approximately 75 billion tons/year (Pimental et al. 1995).

The net loss of soil has both on-site and off-site consequences as summarized by Pimental et al. (1995). In croplands, the diminished fertility due to topsoil erosion requires fertilization or results in diminished yields, creates pressure to deforest new areas as fertility of existing cropland decreases, and results in the loss in water holding capacity of soils. Fertilization, in turn, often has its own consequences. Most fertilizers rely on fossil fuels to create, ship, and apply the material and the applied fertilizer has the potential for creating downstream water quality concerns. The additional water use required because of diminished soil retention taxes another critical resource. In forestlands, soil loss can change species composition, diminish water-holding capacity, and speed desertification. In suburban and urban areas, soil loss can reduce the ability of soils to sustain vegetative cover and trees helpful in addressing air, water, heat, and sound pollution.

Fine sediments derived from erosion of soil are disproportionately responsible for degradation of surface waters (Nelson and Logan 1983; Dong et al. 1984). Eroded soil impairs water quality (Sekely et al. 2002; Sharpley et al. 1994; Pote et al. 1996) to the point that drinking water supplies, aquatic environments, and opportunities for recreation are threatened. Eroded soil often harms aquatic environments by inhibiting light penetration (Yamada and Nakamura 2002), by siltation of rivers (Reiser 1998) and reservoirs (Williams and Wolman 1984), by eutrophication of waterways, lakes, and seas (Rabalais et al. 1999), and by contamination (Tarras-Wahlberg and Lane 2003). In 2000, the US Environmental Protection Agency reported that siltation debilitated 12% of the stream reaches assessed by states and tribes and was responsible for 33% of impairments to beneficial use (USEPA 2000). In areas where wind is an important process of erosion, the transported fine material can be a health problem, foul equipment, and cause abrasion requiring the repainting of structures (Lyles 1985).

History shows that civilization can collapse as the soil resource is depleted (Montgomery 2007; Diamond 2005; Hyams 1952). Plato ascribed the poor soils of his native Attica to erosion after land clearing and his view of the causative factors of poor soil was shared by Aristotle (Montgomery 2007). Loss of production associated with soil loss and degradation ultimately affected the stability of the Greek civilization as it did the Romans later. Lowdermilk (1953) describes a trail of societies from Judea to Syria to China where poor stewardship of the land and resulting erosion led indirectly to conquest or societal discord. More recent examples of societal dislocations (famine and migration) associated with soil erosion and land degradation include the Dustbowl of the 1930s, the Sahel of the 1970s, and Haiti.

25.1.2 Tools for Measuring Soil Erosion

Critical to the understanding and quantification of soil erosion are tools for its measurement. Erosion pins, sediment accumulated in reservoirs, measured sediment concentration in streamflow, photographic techniques, and soil tracers each have their usefulness and limitations. Sediment budgets (Dietrich and Dunne 1978) are often a basis for quantifying the various processes and paths that move soil on the landscape and result in local loss (erosion) and local gain (deposition) of soil.

A particularly useful tool for measuring soil erosion is a conservative tracer of the soil particles, especially when the tracer is relatively easy to measure. Important considerations in the use of a tracer are that the concentration of the tracer is relatively uniform; adsorption of the tracer to soil is strong and quick; variation in adsorption to various sizes or mineralogic/organic constituents is minor or can be accounted for; and methods exist to measure the tracer.

The best known of the tracers for estimating soil erosion are natural and anthropogenic radionuclides. The anthropogenic radionuclides found on the landscape were produced largely by atmospheric nuclear bomb testing and the fallout was distributed globally. The list of fission products is extensive, although many of these radionuclides are too short-lived to be useful tracers of soil erosion. Of the longer-lived fission products, the best known is ^{137}Cs, but the list of other useful tracers includes ^{134}Cs, ^{238,239,240}Pu, and ^{241}Am as minute solid particles or sorbed to soil particles; and ^{3}H and ^{90}Sr as soluble tracers. The naturally-occurring radionuclides are produced by various nuclear reactions, or uranium or thorium decay chains (Porcelli and Baskaran 2011) and include ^{7}Be, ^{210}Pb and a few others. ^{137}Cs, ^{7}Be, and ^{210}Pb are each suitable as particle tracers because they have a global distribution, adsorb efficiently to soil particles and thus move with soil, and are relatively easily measured.

^{137}Cs is the most widely used radionuclide tracer for soil erosion (Ritchie and McHenry 1990). For years, Ritchie and Ritchie (2008) maintained a bibliography of publications that utilized ^{137}Cs in the study of soils and sedimentation. Figure 25.1, redrafted from Ritchie and Ritchie (2008) and updated here to include papers published after December 15, 2008, illustrates how widespread the use of ^{137}Cs as a tracer has been. There are a total of about 4,500 Cs references with the vast majority of the papers following the Chernobyl accident in 1986. In comparison, there are about 2,700 references to the use of ^{210}Pb in studies of soils and sedimentation. The use of ^{210}Pb in such studies now exceeds the use of ^{137}Cs. The use of ^{7}Be as a tracer in the context of soils and sediment is relatively new and has resulted in about 90 papers to date. It should be noted that substantially less than half of the total number of papers have used the respective tracer to quantify soil erosion.

25.1.3 Summary of Contents of Book Chapter and the Approach Used

This chapter focuses primarily upon the use of anthropogenic and naturally-occurring radionuclides to study soil erosion processes and to quantify rates of soil erosion. Many other processes affect soil and sediment transport and deposition and other radionuclides used in those studies are detailed in other chapters of this collection. Here we devote much of our attention to the anthropogenic radionuclide ^{137}Cs but we also look at other radionuclide tracers in part to show which radionuclides may be the most suitable for given applications. Specifically, we describe the source of the radionuclides; their characteristics, deposition, sorption, and transport; the methods of measurement; the assumptions associated with their use as

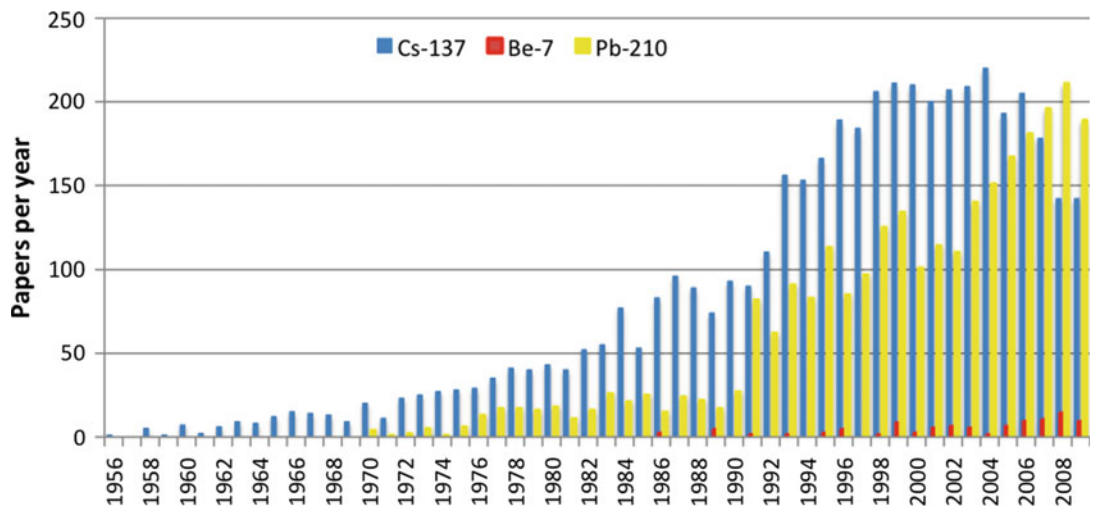

Fig. 25.1 The annual number of papers utilizing ^{137}Cs, ^{210}Pb, and ^{7}Be in chronologic, geomorphic and sedimentologic studies. The total number of ^{137}Cs papers is now about 4,500. Modified and updated from Ritchie and Ritchie (2008)

tracers; the models used to estimate erosion with the tracers; the relative merits of different models and tracers for investigating soil erosion; recent applications of radionuclides in erosion studies; and foreseeable changes in the use of tracers and the tracers used.

25.2 Background

25.2.1 Radionuclides in the Environment

25.2.1.1 Sources of ^{137}Cs, ^{7}Be, ^{210}Pb, and ^{239,240} Pu

Radionuclides that have been used in studies of soil erosion on decadal time scales or less include ^{134}Cs, ^{7}Be, ^{210}Pb, and ^{239,240}Pu but the most widely known of these is ^{137}Cs ($t_{1/2}$ = 30.1 years). ^{134}Cs ($t_{1/2}$ = 2.06 years), ^{137}Cs, ^{239}Pu ($t_{1/2}$ = 4,110 years) and ^{240}Pu ($t_{1/2}$ = 6,537 years) are present on the global landscape largely as a result of anthropogenic fallout from thermonuclear weapons testing primarily during the period 1954–1968 (Fig. 25.2). In parts of Europe, ^{137}Cs fallout from the nuclear reactor accident at Chernobyl in 1986 is superimposed on the global signal of fallout and the Pu isotopic signatures from stratospheric fallout and from Chernobyl are different from each other (Ketterer et al. 2011; Hong et al. 2011). Other accidental releases of Cs isotopes have created local zones of contamination. ^{210}Pb ($t_{1/2}$ = 22.3 years) is delivered to the landscape as a result of the decay of gaseous ^{222}Rn in the ^{238}U decay chain. In that chain, ^{226}Ra in soils and rock decays to ^{222}Rn ($t_{1/2}$ = 3.8 days) which is released to the atmosphere and undergoes a series of short-lived decays to ^{210}Pb which, as a particulate, is delivered to the landscape by wet and dry fallout. This ^{210}Pb is termed excess ^{210}Pb ($^{210}Pb_{xs}$) (Fig. 25.2). However, some ^{222}Rn that occurs in the soil is trapped in mineral matter or unable to escape to the atmosphere during its 3.8 day half-life, and its decay builds the supported pool of ^{210}Pb in the soil (supported ^{210}Pb). ^{7}Be ($t_{1/2}$ = 53.3 days) is produced by cosmic ray spallation of nitrogen (90%) and oxygen (10%) in the troposphere and stratosphere (Kaste et al. 2002; Kaste and Baskaran 2011) and then it is removed from the atmosphere and is delivered to the landscape often during large thunderstorms (Dibb 1989).

^{137}Cs atmospheric fallout is at present very small and the negligible amount, if any, is due to eolian resuspension of near-surface soil particles with adsorbed ^{137}Cs. ^{210}Pb concentration is highest in air originating over continental regions (Turekian et al. 1983; Paatero and Hatakka 2000) and the activity of ^{210}Pb in the atmosphere decreases with altitude (Kownacka 2002) consistent with the sources of the radionuclide in soil and rock at the earth surface. ^{7}Be is produced through spallation interactions of atmospheric O and N nuclei and the nucleonic component of the atmospheric cascade induced by galactic cosmic rays (Dorman 2004) (Fig. 25.2). Sugihara et al. (2000) suggest that 70% is produced in the stratosphere. ^{7}Be is also added to the troposphere from the stratosphere by mixing along the polar front and the subtropical jet and by mixing in large synoptic storms (mid-latitude cyclones and hurricanes). ^{7}Be concentration increases with altitude given the substantial reservoir in the stratosphere where concentrations may be an order of magnitude higher than in the upper troposphere

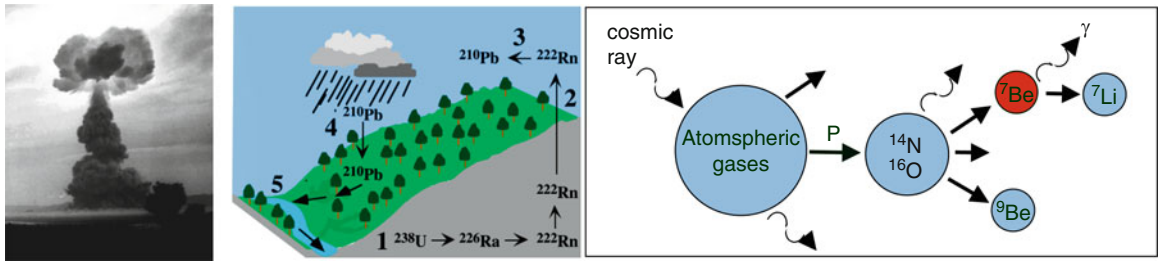

Fig. 25.2 Schematic illustration of fallout radionuclide sources used in erosion studies of decadal or shorter time scales. *Left figure* is a photograph of an atmospheric bomb test, the main source of global radioactive Cs and Pu fallout. Photo from: http://www.nv.doe.gov/news&pubs/photos&films/atm.htm. The *middle figure* illustrates excess ^{210}Pb fallout. The figure on the *right* illustrates the production of ^{7}Be by cosmic ray spallation of oxygen and nitrogen in the stratosphere

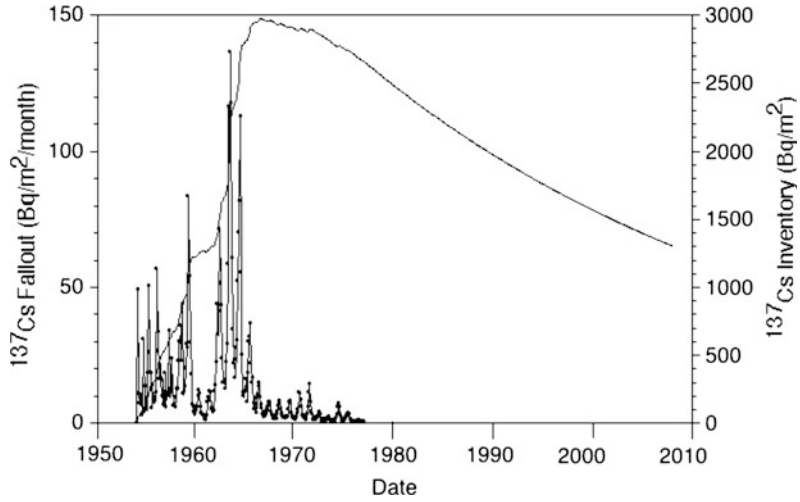

Fig. 25.3 ^{137}Cs fallout (Bq m^{-2} month^{-1}) calculated as 1.45 times the average ^{90}Sr monthly fallout at the US DOE monitoring sites (Birmingham, AL; Los Angeles, CA; San Francisco, CA; Denver, CO; Coral Gables/Miami, FL; Argonne, IL; International Falls, MN; Columbia, MO; Helena, MT; New York, NY; Williston, ND; Wooster, OH; Tulsa, OK; Medford, OR; Columbia, SC; Vermillion, SD; and Green Bay, WI). Data from the Health and Safety Laboratory (1977). Also shown is the calculated ^{137}Cs inventory (Bq m^{-2}) assuming that all the fallout to the soil surface remains in the soil and is subject only to radioactive decay. Chernobyl fallout is not included in this calculation

(Lal and Peters 1967; Dutkiewicz and Husain 1985; Lal and Baskaran 2011). There appears to be some seasonality of the concentrations of ^{210}Pb and ^{7}Be in the atmosphere with the highest values in late spring and summer (Turekian et al. 1983; Baskaran et al. 1993; Caillet et al. 2001). Valles et al. (2009) show a 2–3-fold variation in monthly concentrations of ^{7}Be and ^{210}Pb. Greater emissions of ^{222}Rn from snow-free areas and dry soils are thought to increase atmospheric concentrations of ^{210}Pb during summer (Olsen et al. 1985; Caillet et al. 2001). The seasonal peak in ^{7}Be concentration in late spring and summer (e.g. El-Hussein et al. 2001) is thought to be caused by enhanced mixing of stratospheric air into the troposphere. Longer term fluctuation in ^{7}Be fallout has been tied to variations in the flux of cosmic galactic primary radiation caused by the 11-year sunspot cycle (Azahra et al. 2003; Kikuchi et al. 2009).

^{137}Cs (+), ^{7}Be (2+), and ^{210}Pb (2+, 4+) are strongly chemically active, so they rapidly become associated with aerosols and particles (0.7–2 μm; Ioannidou and Papastefanou 2006) and are delivered from the atmosphere to the earth surface predominantly in precipitation (Olsen et al. 1985). Snow is more efficient than rain at removing radionuclides from air (McNeary and Baskaran 2003; Ioannidou and Papastefanou 2006) and wet precipitation is more efficient than dry precipitation. Residence times in the troposphere are estimated to be 22–48 days (Durana et al. 1996) for ^{7}Be and just a few days for the aerosols carrying the ^{210}Pb (Tokieda et al. 1996). ^{137}Cs also has a short residence time partly because the source of the radionuclide is now resuspension of soil particles that are coarser (Papastenfanou et al. 1995; Ioannidou and Papastefanou 2006). During the weapons testing era, ^{137}Cs residence time in the atmosphere was longer (~1–10 years) than it is today because of its injection into the stratosphere (Joshi 1987).

Although the first nuclear detonation was in 1945, ^{137}Cs was first detected in fallout in 1951 and over most of the globe it was below detection prior to about 1954, peaked in about 1963, and was effectively below detection by 1983 (Cambray et al. 1985) (Fig. 25.3). The data in Fig. 25.3, for the most part, are not based on actual ^{137}Cs fallout data because ^{137}Cs was not routinely monitored during the 1950–1983 time frame. Instead, ^{90}Sr fallout was usually monitored and ^{137}Cs fallout is inferred by assuming a ^{137}Cs/^{90}Sr ratio in the bomb fallout (Health and Safety Laboratory 1977; Robbins 1985). This ratio has been estimated to range from 1.4 to 1.65 and is characteristic of production rates of the isotopes and is independent of location. The $^{239+240}$Pu depositional fluxes are less well known because certain data (i.e., the ratios of

plutonium to ^{137}Cs, ^{90}Sr) are still classified by the U.S. Government. More recently, for example during the monitoring of Chernobyl fallout, deposition of ^{131}I was monitored and the deposition of all other radionuclides was calculated from the ^{131}I deposition density values using the relationships calculated by Hicks (1982). The overall geographic patterns of ^{90}Sr and $^{239+240}$Pu differ slightly from those for ^{137}Cs and ^{131}I primarily due to the differences in the nuclear fuel used in different tests, the size of the particles associated with the radionuclides, and the directions of travel of the clouds of radioactive particles from each test. The overall deposition of ^{90}Sr was very similar to that of ^{137}Cs. For most of the regions in the United States, the activity of ^{137}Cs was 10–20 times the activity of $^{239+240}$Pu deposited (Beck 1999; CDC 2006).

Because of the temporal variability with a peak ^{137}Cs fallout activity in 1963, that peak is often used as a time horizon in sediments to indicate the time of deposition of that layer of sediment. Linear sedimentation rates (cm year^{-1}) are then simply calculated as the depth of the layer (cm) divided by the time in years since 1963. The mass flux deposition rates (g cm^{-2} year^{-1}) are calculated as the cumulative dry mass of sediment above the 1963 time horizon divided by the cross sectional area of the sediment core divided by the time in years since 1963 until the date of coring (Walling and He 1997a, b; Goodbred and Kuehl 1998).

Inspection of Fig. 25.3 shows that the ^{137}Cs depositional flux was highly variable, reflecting the times of atmospheric testing. There are peaks in fallout observed each year between 1954 and 1959, and much larger peaks in 1962, 1963 and 1964. The maximum global fallout of radioactive nuclides occurred in Spring 1964, but because most field data cannot resolve the 1962 to 1964 fallout peaks, the position of the maximum in ^{137}Cs is often assigned a date of 1963 (1964 in the southern hemisphere). In the late 1960s to mid-1970s, fallout decreased considerably, but the seasonal cycle reflecting precipitation can be seen through the 1970s.

As a result of the nuclear accident at Chernobyl in 1986, additional ^{137}Cs fallout occurred in some areas of Europe. It is estimated that the Chernobyl accident released from 10 to 16% as much ^{137}Cs to the environment as was emitted from all nuclear weapons tests (Flavin 1987). Little Chernobyl fallout occurred over North America (Roy et al. 1988). Note the much higher levels of ^{137}Cs deposition from Chernobyl than from stratospheric fallout (compare Figs. 25.3–25.5). For example, the *lowest* contours on the Europe map following Chernobyl are ~2 kBq m^{-2} (light yellow in Fig. 25.4) De Cort et al. (1998) whereas in Fig. 25.3 the *largest* fallout values in the US following bomb testing are ~3,000 Bq m^{-2} (3 kBq m^{-2}). Monthly deposition values are 20–30 times less than the lowest fluxes deposited from Chernobyl. The highest Chernobyl fluxes are ~1,480 kBq m^{-2}, a value 10,000× larger than the peak monthly fallout from atmospheric weapons testing (~140 Bq m^{-2} month^{-1}) and a value at least 100× larger than the inventory in US soils (8–13 kBq m^{-2}, Fig. 25.5). Delivery of ^{137}Cs from the atmosphere is again currently near zero (Quine 1995). The much higher deposition of Chernobyl-derived ^{137}Cs over northern Europe is significant, because in these locations it has swamped the prior global fallout signature and has had the effect of "resetting" the ^{137}Cs soil erosion clock to 1986 because downcore soil inventories and soil activities near the soil surface are now dominated by Chernobyl-derived ^{137}Cs. This is not the case over most of the rest of the world, as the ^{137}Cs fallout from Chernobyl was minimal (Department of National Health and Welfare 1986). Consequently, the current distribution of ^{137}Cs in soils in northern Europe is dominated by Chernobyl fallout and in the US by stratospheric fallout. This resulted because Chernobyl was characterized by the relatively intermittent release of a full range of radionuclides at relatively low temperatures with very heavy local fallout from tropospheric transport. Weapons testing fallout was at a high temperature with more uniform stratospheric transport, longer residence times, and with much less pronounced local fallout (Joshi 1987). Pu atom ratios can be used to distinguish between Chernobyl and stratospheric fallout. The ^{240}Pu/^{239}Pu atom ratio was about 0.38 in Chernobyl fallout and 0.18 in stratospheric fallout (Ketterer et al. 2011). Further, the distribution of Pu from Chernobyl was much more localized than was ^{137}Cs. Pu isotopes were specifically associated with non-volatile fuel particles (Mietelski and Was 1995) whereas ^{137}Cs volatilized in the reactor accident and was more widely dispersed over much of northern Europe and Russia. ^{7}Be and ^{210}Pb deposition on the other hand continues as natural processes continue to produce these radionuclides.

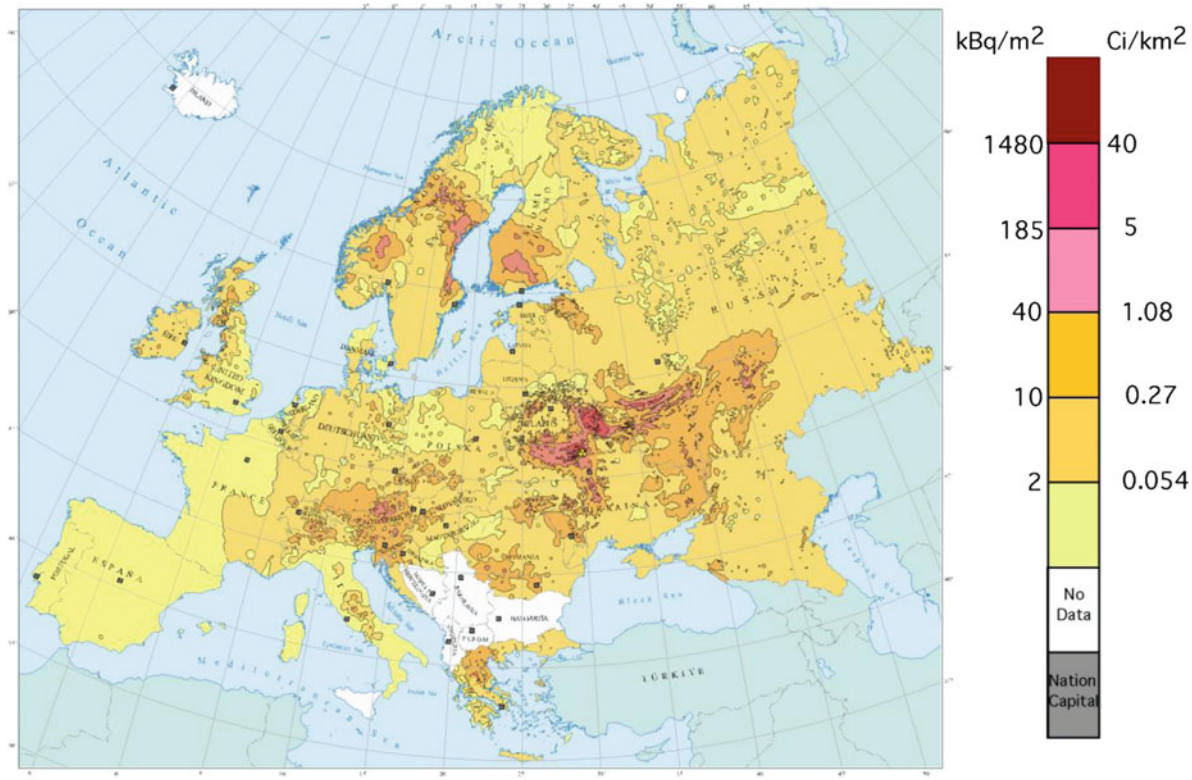

Fig. 25.4 ^{137}Cs fallout deposition over Europe following the Chernobyl accident. Modified from EC/IGCE, Roshydromet (Russia)/Minchernobyl (Ukraine)/Belhydromet (Belarus) (1998)

25.2.1.2 ^{137}Cs, ^{7}Be and ^{210}Pb in Precipitation

Deposition of radionuclides occurs both by dry and wet fall. The vast majority of ^{7}Be falls in association with rainfall. Workers have reported dry fall as making up 3–10% of total fallout (Wallbrink and Murray 1994; McNeary and Baskaran 2003; Salisbury and Cartwright 2005; Ioannidou and Papastefanou 2006; Sepulveda et al. 2008). Dry deposition of ^{210}Pb appears to be more variable than ^{7}Be because of the importance of resuspended soil and dust in contributing to the flux (Todd et al. 1989). The monthly atmospheric depositional flux (wet plus dry) of both ^{7}Be and ^{210}Pb varies by about a factor of 5 over the course of a year (Matisoff et al. 2005) but exhibits a maximum in the spring (Turekian et al. 1983; Olsen et al. 1985; Dibb 1989; Todd et al. 1989; Robbins and Eadie 1991; Koch et al. 1996; Baskaran et al. 1997) and represents the variability in the quantity of precipitation (Turekian et al. 1983; Koch et al. 1996; Baskaran et al. 1997) and, to a lesser extent, the seasonality in stratospheric ^{7}Be production and troposphere-stratosphere exchange (Turekian et al. 1983; Todd et al. 1989; Koch et al. 1996). ^{7}Be and ^{210}Pb deposition during precipitation events is well correlated to precipitation amount (Caillet et al. 2001; Ciffroy et al. 2003; Su et al. 2003) reflecting the fact that wet fall is a dominant delivery mechanism. Caillet et al. (2001) found that ^{7}Be deposition was slightly better correlated with precipitation than ^{210}Pb deposition ($r^2 = 0.66$ for ^{7}Be vs. 0.55 for ^{210}Pb). The better correlation with ^{7}Be is due to the fact that more of the ^{210}Pb comes from dry deposition and ^{7}Be is often derived from the stratosphere during large thunderstorms. Quine (1995) reported that ^{137}Cs delivery from global fallout was also highest in spring and early summer. Callender and Robbins (1993) observed an annual cycle of ^{137}Cs deposition in the high sedimentation environment of Oahe Reservoir (South Dakota, USA).

Given the correlation between fallout and precipitation amounts during events, it is not surprising that the annual fallout of ^{137}Cs, ^{7}Be and ^{210}Pb is correlated to

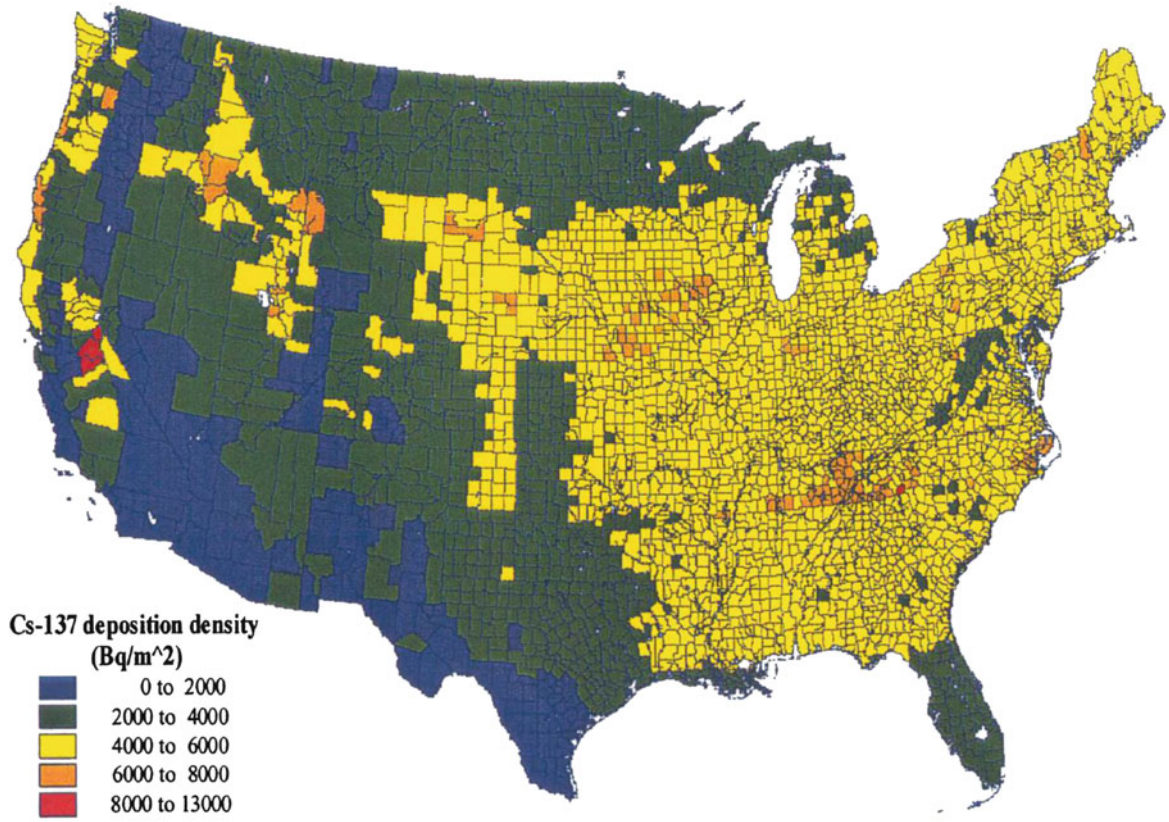

Fig. 25.5 ^{137}Cs depositional flux in the continental United States from global fallout (CDC 2006)

annual precipitation. In most places, the precipitation-normalized annual depositional fluxes have remained constant (Baskaran 1995). Ritchie and McHenry (1978) noted that the variation in ^{137}Cs inventory in the northcentral US was best explained by mean annual precipitation. Rowan (1995) found that variation in mean annual precipitation (900–2,000 mm) explained 75% of the variation in ^{137}Cs inventory in the Exe basin in the United Kingdom. Lance et al. (1986) found a linear relationship between the inventory of ^{137}Cs in soils and average annual precipitation in the southern USA. Baskaran et al. (1993) observed that ^{210}Pb fluxes increased with precipitation and Gallagher et al. (2001) found that ^{210}Pb inventory was significantly higher on the wetter west coast of Ireland than on the east coast. Our survey of annual delivery of ^{7}Be reported by workers (Turekian et al. 1983; Dibb 1989; Papastefanou and Ionannidou 1991; Baskaran et al. 1993; Caillet et al. 2001; Ayub et al. 2009) as compared to annual precipitation shows a strong correlation: $r^2 = 0.72$ (Fig. 25.6).

The fallout of ^{137}Cs over the globe as indicated by soil inventories is higher in the mid-latitudes than equatorial areas, and higher in the Northern Hemisphere than in the Southern Hemisphere (Stokes and Walling 2003; Walling et al. 2003). Collins et al. (2001) found inventories that were almost an order of magnitude higher in mid-latitudes of the Northern Hemisphere. Figure 25.7 illustrates the general pattern of inventories by latitude across the globe and Fig. 25.8 illustrates the reconstructed global fallout of ^{137}Cs as of 1970 indicating both the localized fallout from the test sites and the global fallout. McHenry et al. (1973), summarizing several studies, noted that fallout in the USA increased to the north and to the east (Fig. 25.5). Sarmiento and Gwinn (1986) developed a semi-empirical model for the deposition of ^{90}Sr (and hence ^{137}Cs) that is based on latitude, time since 1954, and the monthly precipitation. The distribution

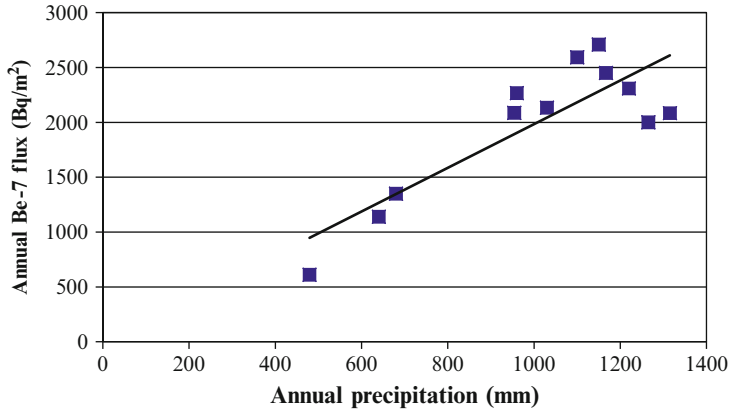

Fig. 25.6 Linear relationship between ^{7}Be depositional flux and annual precipitation

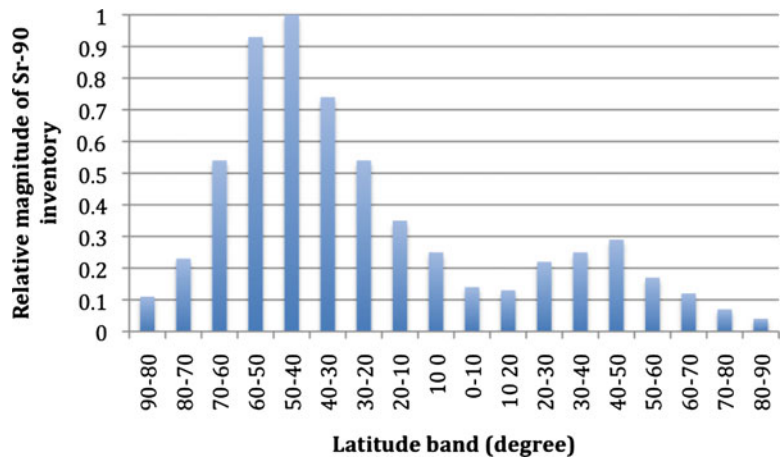

Fig. 25.7 Variation in bomb-derived ^{90}Sr (a surrogate for ^{137}Cs) by latitude band (from Stokes and Walling 2003)

of bomb-derived ^{137}Cs fallout over the globe is relatively smooth in contrast to the Chernobyl fallout (compare Figs. 25.4 and 25.5) because the global fallout signal is due to a series of nuclear explosions that reached into the stratosphere allowing ^{137}Cs to be well mixed in the atmosphere. In contrast, the plume of radioactive debris from Chernobyl did not extend higher than a few km into the atmosphere and thus prevailing winds, and then rainout, determined the pattern of fallout. ^{239,240}Pu was also vaporized during bomb testing and its global distribution is similar to that of ^{137}Cs. However, this did not occur during Chernobyl, so the Pu was delivered as fine particulates and therefore its distribution was not widespread (Mietelski et al. 1996; Ketterer et al. 2004; Brudecki et al. 2009). Global fallout flux of ^{210}Pb is summarized in Baskaran (2011). The inventories of ^{210}Pb are lower in the Southern Hemisphere than the Northern Hemisphere because of the smaller percentage of land area. The radon flux from the oceans is negligible compared to the continents (Turekian et al. 1977) thus with less continental area in the Southern Hemisphere there will be a lower atmospheric concentration and less deposition of ^{210}Pb. ^{7}Be inventories should be similar in both hemispheres because of its stratospheric source.

25.2.1.3 ^{137}Cs,^{7}Be and ^{210}Pb in Soils

Once the radionuclides ^{137}Cs, ^{7}Be and ^{210}Pb reach the earth surface, they rapidly sorb to the mineral grains and organic materials of soil particles (Tamura and Jacobs 1960). Cs fixation to soil material depends strongly on soil composition and mineralogy. There is a complicated pattern of preferred sorption of radionuclides to finer particle sizes and to organic materials (He and Walling 1996; Wallbrink and Murray 1996; Motha et al. 2002) and clays (Hawley et al. 1986;

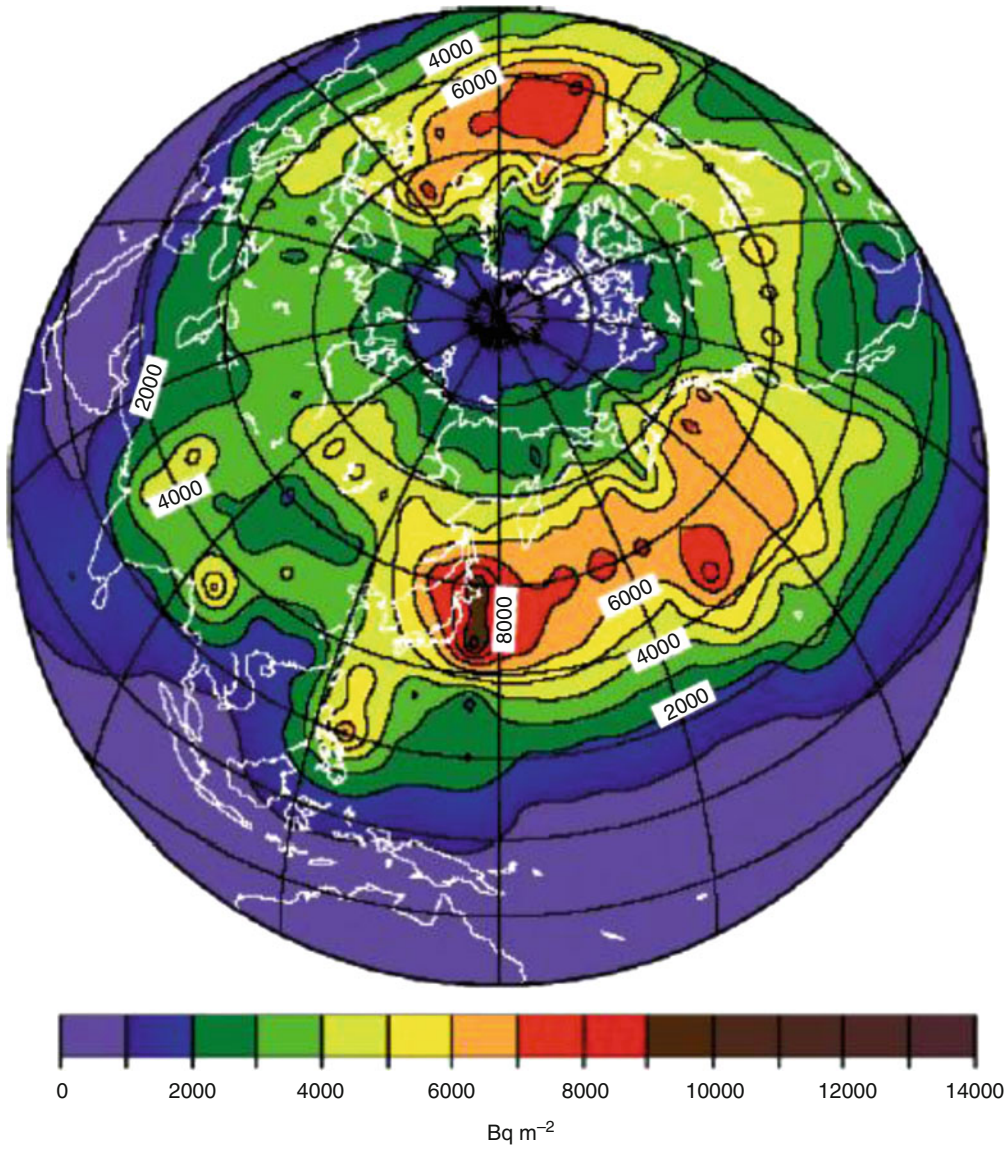

Fig. 25.8 Global distribution of bomb-derived ^{137}Cs fallout illustrating high fallout near testing sites and a strong latitudinal distribution (from Aoyama et al. 2006)

Wang and Cornett 1993; Balistrieri and Murray 1984). ^{137}Cs is a 1+ cation and its sorption exceeds that of all other alkali ions (Schultz et al. 1959). Lomenick and Tamura (1965) suggested that the adsorption is almost non-exchangable. Riise et al. (1990) estimated that less than 10% of Cs was leachable. ^{7}Be reaches the earth surface as a Be^{2+} cation with high charge density which makes it prone to adsorption. ^{210}Pb likewise reaches the surface as a 2+ or 4+ cation and is rapidly adsorbed. Partition coefficients, K_d, for these radionuclides are ~10^5 (Olsen et al. 1986; You et al. 1989; Hawley et al. 1986; Steinmann et al. 1999) indicating that these radionuclides are sufficiently particle-bound that they are suitable for tracing erosion, transport, and deposition of soil.

There are, however environments in which ^{137}Cs might fail as a conservative particle tracer. Some previous studies of radiocaesium in soils have failed because K_d values have been derived under conditions very different from those in situ. The partitioning of Cs

in organic-rich soils is reversible and the partition coefficients can be low. Where the soils are peaty or podzolic, the mobility of cesium is considerably greater than in other soils (Sanchez et al. 1999). In acidic soils in coniferous forests in N. Europe Dorr and Munnich (1989) found that Cs migrated faster than ^{210}Pb and suggested that chemical exchange was occurring between the organic and hydrous phases. It is generally believed that radiocaesium retention in soils and sediments is due to the presence of a small number of highly selective sites. Cremers et al. (1988) found that strong Cs adsorption by the solid phase was regulated by the availability of frayed edge sites on illite and is inhibited by the presence of competing poorly hydrated alkali cations (K^+ or NH_4^+). Where geochemical migration of Cs is significant, workers should turn to alternatives such as Pu isotopes.

In soil, cesium has a low mobility; the majority of cesium ions are retained in the upper 20 cm of the soil surface and usually they do not migrate below a depth of 40 cm (Korobova et al. 1998; Matisoff et al. 2002a). For example, vertical migration patterns of ^{137}Cs in four agricultural soils from southern Chile indicated that approximately 90% of the applied cesium was retained in the top 40 cm of soil and as much as 100% was found in the upper 10 cm (Schuller et al. 1997).

^{137}Cs uptake by plants also affects its downcore migration. Clay and zeolite minerals strongly bind cesium cations in interlayer positions of the clay particles and therefore reduce the bioavailability of ^{137}Cs and its uptake by plants (Paasikallio 1999). Plant uptake of ^{134}Cs in a peat soil was decreased by a factor of 8 when zeolites were added (Shenber and Johanson 1992).

The kinetics of sorption are less understood, but Baskaran and Santschi (1993) reported that approximately 80% of ^{7}Be became associated with particulates within an hour of a rainfall event. In a study where ^{134}Cs was applied in solution to the surface of soils, it was adsorbed in the upper 2.5 cm of the soil (Owens et al. 1996). These results largely mimic the findings of Rogowski and Tamura (1970) who applied ^{137}Cs to the soil surface and also found penetration of only a few cm. This modest penetration during infiltration suggests a timeframe for adsorption of up to 10 min if typical rates of infiltration for these silty sand soils are used.

Some proportion of the radionuclide fallout is retained on vegetation. Doering et al. (2006) observed that 18% of ^{7}Be was retained on vegetation whereas only about 1% of $^{210}Pb_{xs}$ was retained on vegetation. These differences almost surely reflect the much shorter halflife of ^{7}Be than any differences in affinity for organic material. Very little ^{137}Cs is typically on vegetation today because of the negligible fallout. Plants may also take up radionuclides from soil. Coughtrey and Thorne (1983) supposed that plant uptake could result in a 0.2% loss in ^{137}Cs per year. Numerous studies have shown that radioactive contaminants move through the food chain and can exceed health standards (Davis 1986; Revelle and Revelle 1988). For example, mushrooms have been reported to uptake as much as 50% of the ^{137}Cs inventory in the soil and moose, caribou, sheep and milk consumption have all had radioactive residues that restrict their consumption (Korky and Kowalski 1989).

25.2.1.4 Radionuclide Profiles in Undisturbed Soils

The simplest profile of the set of radionuclides most commonly used in soil erosion studies may be that of ^{7}Be (Fig. 25.9; see also Kaste and Baskaran 2011). From a peak concentration at the surface, it decreases exponentially down core to non-detectable values below 2–3 cm (Bonniwell et al. 1999; Wilson et al. 2003; Doering et al. 2006). In the case of ^{7}Be, some fraction is associated with the vegetation growing on the surface (Doering et al. 2006 reported 18%) or associated with organic litter. The half-life of ^{7}Be is just 53.3 days thus there is a relatively brief period to mix/move the radionuclide downward before the radionuclide decays (Walling et al. 2009). Only very rarely has ^{7}Be been measured deeper than a couple of cm in the soil. Kaste et al. (1999a, b) noted a second down-profile peak in activity that they hypothesized might be caused by subsurface pipeflow quickly taking the ^{7}Be cation to depth before sorption.

The next simplest profile may be that of ^{210}Pb (Figs. 25.9 and 25.10). As with ^{7}Be, $^{210}Pb_{xs}$ is delivered by wet and dry fallout to the surface and mixed downward in the soil profile. In the case of ^{210}Pb however, there is both the atmospherically derived $^{210}Pb_{xs}$ and the steady background ^{210}Pb activity (called supported ^{210}Pb) maintained by continuous in

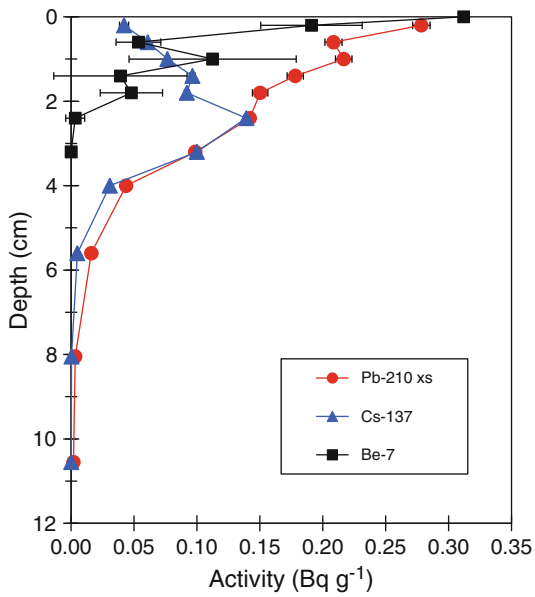

Fig. 25.9 The distribution of radionuclides ^{7}Be, ^{137}Cs, and ^{210}Pb$_{xs}$ in this upland soil from near Corwin Springs, Montana, USA is characteristic of undisturbed soils. ^{7}Be activity is highest at the surface and little is found below 3 cm. ^{137}Cs displays a subsurface peak in activity, in this case between 2 and 3 cm of depth, and no radionuclide activity below 10 cm. ^{210}Pb$_{xs}$ displays a surface peak in activity. ^{210}Pb$_{xs}$ activity is negligible below 10 cm (from Whiting et al. 2005)

situ decay of ^{226}Ra in soil and rock (Goldberg and Koide 1962). The surface maximum in activity decreases exponentially downcore to the value of the supported ^{210}Pb. Most ^{210}Pb$_{xs}$ is found in the upper 10 cm of soil (Bonniwell et al. 1999; Doering et al. 2006). The greater penetration of ^{210}Pb$_{xs}$ than ^{7}Be is due to its greater half-life of 22.3 years. With more time to operate, downward migration extends further.

The ^{137}Cs profile is typically more complicated (Figs. 25.9 and 25.10). Over much of the globe, the undisturbed ^{137}Cs profile features a subsurface maximum and then an exponential decrease below that. Very little ^{137}Cs is found below 20 cm (Owens and Walling 1996) in most locales. Unlike the other two radionuclides, the delivery of ^{137}Cs was not steady (Fig. 25.3). It was first detected in fallout in 1951, peaked in about 1963, and was negligible by the early 1980s. In the absence of constant replenishment to the surface, the peak in concentration has migrated below the surface by several cm. In areas receiving significant Chernobyl fallout after the nuclear plant accident in 1986, the distribution of ^{137}Cs from stratospheric fallout is swamped by the Chernobyl fallout so that global fallout can no longer be identified. This interpretation is supported by Pu isotope data which show "hot"

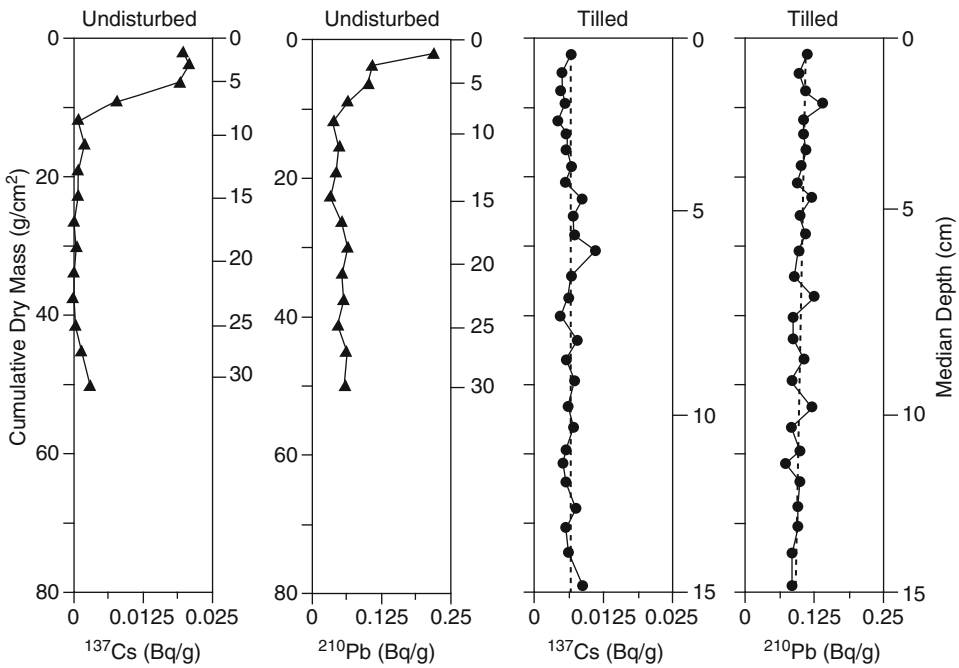

Fig. 25.10 Comparison of ^{137}Cs and ^{210}Pb activities in profiles from undisturbed and tilled soils. Soils collected in Ohio, USA. After Matisoff et al. (2002a, b)

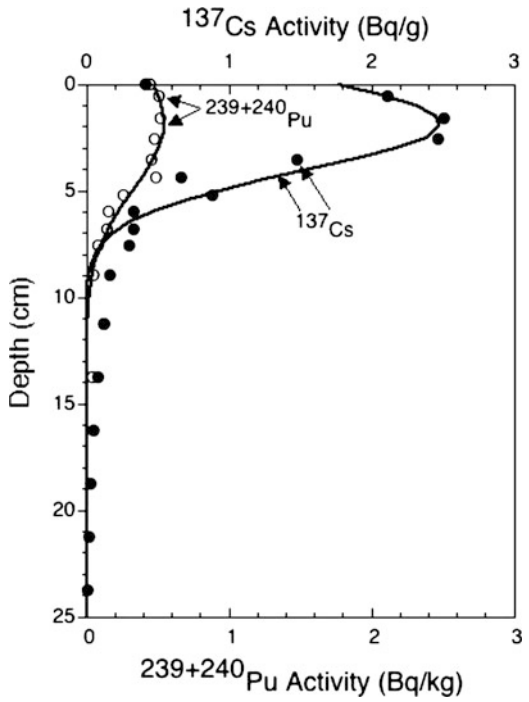

Fig. 25.11 ^{137}Cs and $^{239+240}$Pu data from a core collected in 2008 in Skogsvallen, Sweden and a non-local bioturbation model fit to the data. Note that the Pu is derived from global fallout (as determined from Pu isotopes, not shown here), but the ^{137}Cs is derived primarily from Chernobyl fallout (as determined by its relatively high activity)

Chernobyl-derived Pu particles at depth while stratospheric Pu is found both above and below the Chernobyl Pu and the ^{137}Cs profile mimics the Pu profile (Matisoff et al. 2011). Additional support can be seen in Fig. 25.11, where the Pu profile is from global fallout (as determined from Pu isotopes, not shown here), but the ^{137}Cs is derived primarily (as determined by its relatively high activity) from Chernobyl fallout. (Note the much higher activity of ^{137}Cs in Fig. 25.11 compared to that in Figs. 25.9 or 25.10 indicating a Chernobyl source to the soil collected in Sweden in Fig. 25.11 and a global fallout source to the soils collected in the USA shown in Figs. 25.9 and 25.10.)

25.2.1.5 Downcore Migration of Radionuclides in Soils

The radionuclides delivered to the soil surface are moved downward by soil processes including bioturbation, leaching, diffusion, and translocation. Movement can be enhanced by disturbance such as plowing. The depth of penetration of each radionuclide into the soil is determined by the rate of this downward movement and the half-life of each radionuclide. DeJong et al. (1986) argue for low leachability of ^{137}Cs but some workers have found substantial mobility, particularly in peaty soils. Kaste et al. (1999a, b) report that as pH increases, ^{7}Be can be desorbed.

Since the Chernobyl accident there have been a number of studies on the migration of ^{137}Cs and other radionuclides into the soil. Several authors have reported that ^{137}Cs penetration decreases exponentially downcore (Miller et al. 1990; Walling and Woodward 1992; Wallbrink and Murray 1996; Doering et al. 2006). Several studies have described the downcore transport of ^{137}Cs in terms of a diffusion-advection equation for a sorbed radionuclide (Konshin 1992; Bossew and Kirchner 2004; Shimmack et al. 1997; Rosen et al. 1999). These studies have concluded that the model fails to describe the rapid downward migration of the radionuclides shortly after fallout so that a non-linearity or irreversible sorption process leads to a decrease in the migration rate over time. This may help explain why the ^{239,240}Pu and ^{137}Cs profiles match in Fig. 25.11 even though the ^{239,240}Pu was delivered from stratospheric fallout whereas the ^{137}Cs was delivered from Chernobyl fallout.

Recently it has been suggested that ^{137}Cs transport is facilitated by colloidal transport (Flury et al. 2004; Chen et al. 2005), but colloidal transport in a natural, unsaturated media is small (Honeyman and Ranville 2002; Lenhart and Saiers 2002). Février and Martin-Garin (2005) conducted laboratory experiments that demonstrated retention of anionic radionuclides by microbial activity. Bundt et al. (2000) noted enrichment of radionuclides of Pb, Pu, and Cs at depth in preferential flow paths.

The transport of radionuclides in soils also can be facilitated by burrowing organisms such as earthworms, ants, termites and pocket gophers. Some of these bioturbating organisms are present in soils in numbers that can approach tens of millions per square meter and they actively mix the soil to depths ranging from a few centimeters to a few meters (Johnson et al. 1990; Müller-Lemans and van Dorp 1996; Gabet 2000; Gabet et al. 2003). Darwin (1881) first reported the role of earthworms in facilitating the downward migration of objects by ingesting soil and/or plant

matter at depth and depositing it onto the surface as casts. This mixing style incorporates both random (diffusive) and directed (advective) processes and has been termed "conveyor-belt" feeding (Rhoads and Stanley 1964; Rhoads 1974; Powell 1977) or "non-local" mixing (Boudreau 1986a, b; Robbins 1986). Earthworms have been suggested to be the most important factor controlling the vertical transport of radionuclides in central European soils, with the potential to turn over the top layer of soil within 5–20 years (Müller-Lemans and van Dorp 1996). It is possible to model mixing by bioturbation in soils as a diffusive process and burial as an advection velocity. Kaste et al. (2007) used this approach and reported bio-diffusion mixing coefficients of 1–2 cm^2 $year^{-1}$ in a grassland in California (USA) and from a forested landscape in Australia, and inferred that the more actively bioturbated soils exhibit higher erosion rates. This approach treats the downward migration as a burial velocity and while it may simulate well the downcore profiles, it does not account for the directed recycling of tracer from depth (non-local mixing) as demonstrated by Robbins et al. (1979) using aquatic oligochaetes. Alternatively it is possible to model mixing by bioturbation as a diffusive process and the downward migration as a burial caused by non-local feeding in which the organisms place soil from depth onto the soil surface (Jarvis et al. 2010). Figure 25.11 is an application of the non-local bioturbation model to Chernobyl fallout at a site in Sweden and yields a bioturbation coefficient of 0.1 cm^2 $year^{-1}$ and a feeding rate of 0.002–0.003 $year^{-1}$ over the top 20 cm. In other words, this bioturbation model can account for the burial of the radionuclides by recycling 0.2–0.3% of the top 20 cm of the soil column each year.

25.2.1.6 Effects of Tillage on Soil Profiles

The radionuclide profiles in tilled soils exhibit considerable differences from the profiles in undisturbed soils (Matisoff et al. 2002b). Undisturbed soils show either a surface maximum (^{7}Be, ^{210}Pb) or a near surface peak (^{137}Cs) followed at depth by a decrease to a constant activity (^{210}Pb) or to near zero (^{7}Be, ^{137}Cs) (Fig. 25.9). Plowing of agricultural soils will mix soils to depths of 10–30 cm creating a relatively uniform concentration over the plow depth (Wise 1980 in Martz and deJong 1985; Owens et al. 1996). The distribution of radionuclides in the tilled soils is largely homogeneous because plowing mixes surface soils, which are enriched in radionuclides, with deeper soils, which are depleted in both ^{210}Pb and ^{137}Cs (Fig. 25.10).

Figure 25.12 illustrates a generalized model of the distribution of ^{7}Be, ^{137}Cs and ^{210}Pb in a soil profile. All three isotopes are deposited on the surface through wet and dry fallout. Each radionuclide is distributed differently in the soil because of differences in half-lives, delivery rates, delivery histories, and land use. An undisturbed soil will exhibit higher radionuclide activities near the soil surface, which reflects their surficial input and slow downward transport. The shorter half-life of ^{7}Be compared to ^{210}Pb results in less downward migration of ^{7}Be. Hence ^{7}Be is found only at the soil surface but some ^{210}Pb will migrate down core. In addition, some ^{210}Pb is produced in the soil by in situ decay of ^{222}Rn resulting in some ^{210}Pb activity at all depths in the soil. Because ^{137}Cs had its peak delivery in the early 1960s and almost no delivery before 1951 or since 1975 (or had its peak delivery in 1986 in areas affected by Chernobyl fallout) its activities have a distinct peak at some depth (~10 cm) in the soil. Plowing homogenizes ^{210}Pb and ^{137}Cs within the plowed layer, but because of its short half-life and constant input, ^{7}Be activities are highest at the surface and are homogeneous only immediately after plowing. Because ^{137}Cs fallout occurred at a distinct instance of time, its distribution will remain homogeneous within the soil profile, even after the cessation of plowing. On the other hand, ^{210}Pb, like ^{7}Be, is continuously deposited on the land surface. Its distribution will remain homogeneous if the soil is plowed annually, but it will accumulate at the surface and slowly rebuild a profile with decreasing activity with depth if tillage ceases.

Because ^{7}Be, ^{137}Cs, and ^{210}Pb have different distributions in the soil profile, erosion of the soil to different depths will yield an assemblage of radionuclides in the eroded material that is characteristic of only one depth. Shallow erosion produces proportionally larger amounts of ^{7}Be and ^{210}Pb because these radionuclides are concentrated near the surface. Deeper incision yields progressively less additional ^{7}Be and no additional ^{7}Be below about 1 cm. The

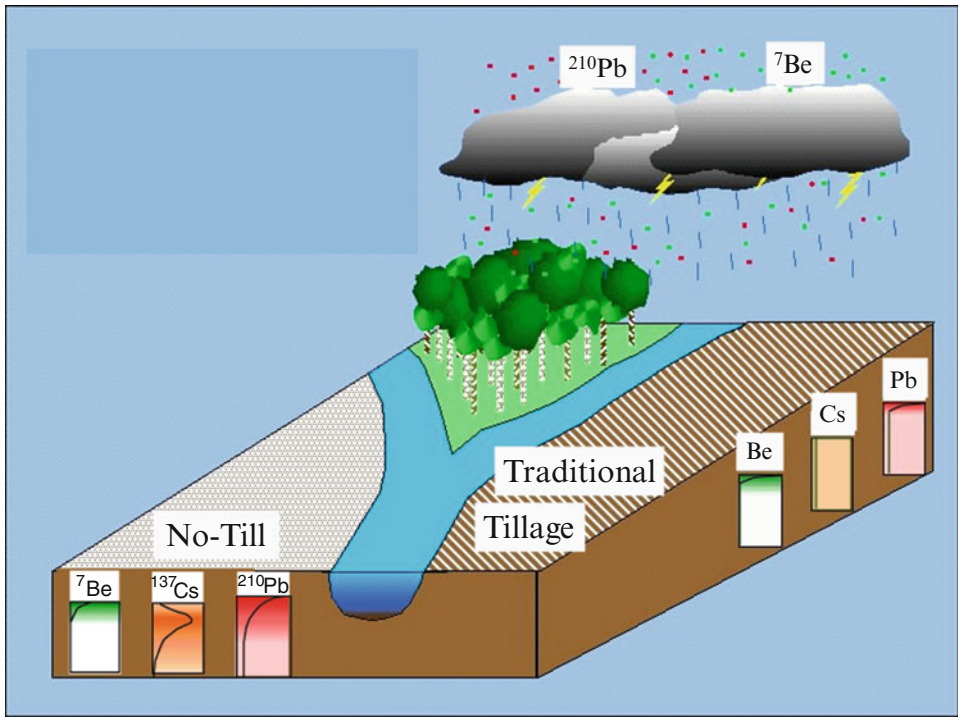

Fig. 25.12 Schematic illustration of soil profiles of ^{7}Be, ^{137}Cs, and ^{210}Pb in undisturbed soils (no-till) and in soils that have been mixed by plowing (traditional tillage)

proportional contribution of ^{137}Cs increases to the depth of its maximum. Erosion below that depth yields incrementally more ^{210}Pb and ^{137}Cs but at progressively decreasing rates. Below some depth in the soil (~15–30 cm), deeper erosion yields little if any additional ^{137}Cs. ^{210}Pb yield continues to grow in correspondence to the constant supported ^{210}Pb activity.

Sediment eroded from a soil will have a radionuclide signature corresponding to the tillage practice and the depth of erosion. Thus radionuclide signatures in suspended sediments can provide a means of tracing particles eroded from the landscape and can identify soil sources and be used to quantify the erosion (Whiting et al. 2001). The distinct distributions of radionuclides permit in principle the use of multiple mass balances to quantitatively estimate the areal extent of rill and sheet erosion and the characteristic depth of erosion associated with each mechanism (Wallbrink et al. 1999; Whiting et al. 1999, 2001). In essence, it is possible to infer the "recipe" for erosion – for example, 1 part sheet erosion to 10 parts rill erosion – on the basis of the total yield of radionuclides and sediment.

25.2.2 Concept of Inventory

The inventory, or standing stock, of a radionuclide represents the total amount of a radionuclide per unit area and is determined by atmospheric delivery, radioactive decay, gain, and loss. Gain typically reflects deposition and loss typically reflects erosion or leaching. In the case of ^{137}Cs, local inventories at stable locations (neither eroding or depositing) are steadily dropping because contemporary fallout to replenish the stock is essentially zero (Fig. 25.3). In 2010, ^{137}Cs inventories are less than half of what they were in 1974, except in areas affected by Chernobyl fallout. ^{210}Pb inventories at stable sites are more or less steady because annual contributions (fallout) to the stock and variation in the delivery from year-to-year are both small compared to the total inventory. For instance, fallout of ^{210}Pb in a typical year represents no more than 3% of the stock of $^{210}Pb_{xs}$. ^{7}Be inventories at stable sites tend to vary over the year due to the variation in delivery with the seasons and the short half-life of 53 days. Individual storms can deliver

>50% of the ^{7}Be inventory particularly when the precipitation event arrives after a period of drought lasting weeks to months.

To use these tracers to quantify erosion or deposition, the amount of the radionuclides in a vertical column of soil (the measured inventory) is compared to the expected amount in the soil profile based upon fallout (the expected inventory). The fundamental idea is that the inventory (stock) of radionuclides will be changed only by additions of radionuclides as wet- and dry-fallout or by sediment deposition or by losses by decay and soil erosion. If the measured inventory is less than the expected inventory, then erosion has occurred and the soil loss is proportional to the ratio of the inventories. If the inventory is greater than the expected inventory, deposition has occurred.

25.2.2.1 The Spatial Variability of Inventory

Erosion and deposition are the primary causes of variation in radionuclide inventory. But other factors also influence the inventory and these include: (1) random spatial variability, (2) systematic spatial variability, (3) sampling variability, and (4) precision in measurement (Owens and Walling 1996). Random spatial variability can be tied to local soil properties, microtopography (i.e. Lance et al. 1986), and localized vegetation distributions. Systematic variation is caused by gradients in precipitation, slope, aspect, windfields, and soil types. Sampling variability is tied to the area of collection with large areas of collection featuring lower variability (Loughran et al. 1988). Owens and Walling (1996) and Foster et al. (1994) estimate variation associated with sampling area is approximately 5%. Finally, measurement precision is an important source of variability and is typically about 10%. Owens and Walling (1996) concluded that local variation in ^{137}Cs inventory was relatively large thus single measurements were unlikely to be appropriate measures of activity. Their summary of their own work and the work of others showed a range in coefficient of variation in Cs inventories of 5–47% with an average value of 29%. For ^{7}Be, Wilson et al. (2003) found a coefficient of variation of 33% in inventories. It might be expected that with the shorter halflife that local variation might add substantially to variability, but that does not appear to be the case.

The change in the inventory of a radionuclide tracer is the basis for estimating soil erosion. In using a radionuclide to quantify erosion, one assumes that the erosion that removes soil also removes the radionuclide tracer. Ideally there is equivalence between the mass loss relative to the potentially erodible material and the radionuclide loss relative to the potentially lost material (inventory). However, radionuclides can still be used to quantify erosion in the absence of equivalence if the tracer loss:soil loss relationship can be quantified. For instance, preferential erosion of certain sized particles enriched in radionuclides might appear to invalidate the assumption of equivalence, but the ability to describe this enrichment will permit determination of erosion.

25.2.3 Time Scales of Utility

Fundamental to the use of tracers to measure rates of soil erosion is the time span over which the loss is calculated. In other words, to determine the rate of erosion using radionuclides, the denominator – time in this case – must be established. Using ^{137}Cs as an example, delivery to the earth surface began around about 1954, peaked in about 1963, and was effectively below detection by 1983 (except in parts of Europe). If we ignore for the moment various other issues, we might reasonably calculate the amount of erosion by measuring the amount of Cs in the soil lost relative to the amount we would expect based upon fallout (accounting for decay). To determine a rate, we do not know anything about the timing of erosion in this interval since deposition so we will assume that the erosion occurred over the period since 1954 when deposition began. In such a scenario, the erosion rate is determined for a period of 56 years (assuming 2010 as the measurement date).

What sets the shortest and longest scales for the use of a radionuclide to estimate erosion? If erosion rate is being determined retrospectively, these are the considerations for the timescale of utility. In the case of a retrospective analysis, the scientist is typically measuring one time the inventory of the radionuclide at a site where erosion occurred and comparing this inventory to the inventory at a reference site without erosion or to the inventory expected given the estimated fallout. The changes in inventory are converted

to soil loss and the rate is determined by the time since deposition.

If repeated measurements of inventory are made and made sufficiently far apart in time, the erosion of soil over shorter time periods can be examined. What is "sufficiently far apart in time?" To estimate erosion a difference in inventory must be measurable. It is typical that analytical errors in activity are at least 10%. In the case of ^{137}Cs, a 10% uncertainty in measured activity when compared to the decay rate, corresponds to a resolution in time no finer than 5 years (~10% of the mean life of the ^{137}Cs). Longer time scales, at least a decade (Walling and Quine 1990), are typically needed to produce measurable changes in ^{137}Cs inventories. In the case of Pb, this finest resolution is about 3 years (~10% of the mean life of ^{210}Pb). For ^{7}Be, the variable flux means that under certain circumstances, the finest resolution is a matter of days or at the scale of individual precipitation events. One factor influencing the timeframe over which changes in inventory can be recognized is the distribution of the tracer in the soil. If the bulk of the tracer is at the surface, significant amounts of the tracer can be removed with a given amount of erosion. Less of the tracer will be removed by the same amount of erosion if the same inventory is distributed more deeply in the soil. In summary, the amount of erosion; the half-life; the history of deposition, erosion, and mixing of the surface fallout into the soil profile; and the precision in measurement are the keys to the timescale of utility for the various radionuclides. Section 25.4, which summarizes the major classes of models for estimating erosion rates using ^{137}Cs and their assumptions, will treat this subject further.

25.3 Collection and Measurement of Samples

25.3.1 Soil Collection

In order to determine soil radioactivity inventories it is necessary to collect intact soil cores and measure vertical profiles of the radioactivity. Since the radioactivity of ^{137}Cs has often migrated downcore to depths of 20 cm or more, push cores, for example the types used by golf courses to examine turf quality, are too short. Accordingly, hammer-driven cores and soil pits are used to obtain deeper cores. If high resolution profiling of the cores is desired, for example to obtain a ^{7}Be profile, then the diameter of the tube needs to be large enough to collect sufficient sample to measure the radionuclide activities in a reasonable counting time. Typical push or hammer cores obtain a 1-in. diameter tube, and by using extension rods the tubes can be collected to a depth of 60-cm or more. However, this type of coring method causes significant (often ~20–30%) compaction of the soil, so that the true depths are poorly known even if they are compaction corrected. Compaction can be minimized by using a larger diameter tube, but it is more difficult to obtain deeper cores with a larger diameter tube. High-resolution soil profiles are easier to obtain from soil pits (Wilson et al. 2003) but the digging and sampling of soil pits is tedious and slower. Alternatively, thin layers of soil may be scraped from the surface of a large area to obtain high resolution vertical profiles (Walling et al. 1999a, b) – a method that is also quite tedious to construct. Regardless of the sampling technique used, it is necessary to know the surface area sampled since radionuclide inventories are expressed as activity per unit area.

After collection, the soil samples need to be dried, ground with a mortar and pestle to a fine texture, placed in standardized geometries, and analyzed by gamma spectroscopy for their radionuclide activities.

25.3.2 ^{137}Cs Measurement

The measurement of ^{137}Cs is accomplished by gamma spectroscopy. ^{137}Cs undergoes β^{-} (negatron) decay and emits gamma energies at 31.82 keV (relative intensity = 1.96%), 32.19 keV (relative intensity = 3.61%), 36.40 keV (relative intensity = 1.31%), and 661.66 keV (relative intensity = 85.21%). The two lowest energy photopeaks usually cannot be baseline resolved, so they are not used. The photopeak at 36.40 keV has been used, but it is not an ideal choice for measurement because the weak gamma in that energy range undergoes significant sample self absorption for which a large correction is necessary (Cutshall et al. 1983), its relative intensity is fairly small, and, depending on what other isotopes are

being analyzed in the same spectrum, that portion of the spectrum may not have good photopeak separation. The photopeak at 661.66 keV is usually used because the relative intensity is much larger, the spectrum background and the efficiency are relatively constant in that part of the spectrum, and there are no other peaks that overlap or interfere. However, the detector efficiency for solid-state detectors is low at that energy requiring large sample sizes or long counting times to acquire a suitable peak for quantitation.

There are several different types of detectors capable of measuring ^{137}Cs. While Si detectors are commonly used for X-ray analyses, their efficiencies are too low at the higher energies needed for ^{137}Cs detection. The most common detectors that can measure the 661.66 keV photopeak of ^{137}Cs include NaI and Germanium (HPGe) semiconductors, although it is possible to use other detectors, such as Cd-Te, Cd-Zn-Te, and Hg-I. These other detectors have an advantage of reasonably good photopeak resolution and peak to Compton ratio while not require liquid nitrogen cooling. Their disadvantage is that for most applications they are too small and have a very low efficiency at 661.66 keV and therefore require counting times that are too long for practical applications. However, larger crystals are being developed and they may eventually replace NaI and HPGe detectors. NaI detectors have the advantages of being relatively inexpensive, have the highest efficiency of all the detectors discussed here, and requiring no liquid nitrogen for cooling. However, the photopeak energy resolution for NaI detectors is very poor and in most samples the ^{137}Cs photopeak is not visually detectable. Quantitation of a non-visual photopeak requires complex peak separation software, and since the peaks are not visually obvious, the use of NaI detectors to measure ^{137}Cs in soils and sediments seems a "bit like magic" or at the very least results in a lack of confidence in the results. High purity germanium detectors (HPGe) provide the easiest, and most accurate quantitation of the 661.66 keV photopeak of ^{137}Cs. These detectors provide excellent energy resolution and peak to Compton ratios over most of the applicable gamma-ray spectrum, so that ^{210}Pb, ^{7}Be, ^{134}Cs, ^{137}Cs and ^{40}K and other gamma-emitting isotopes may all be determined at the same time from a single spectrum. However, they are more expensive than the other types of semiconductors discussed here and they require liquid nitrogen cooling. Other analytical techniques, such as alpha and beta spectroscopy for the determination of ^{210}Pb and ICP-MS for the determination ^{239,240}Pu are discussed in more detail in other chapters (Ketterer et al. 2011).

25.3.3 Calibration and Standards

Calibration of a detector for ^{137}Cs analyses consists of both an energy calibration and an efficiency calibration. The purpose of the energy calibration is to assign the correct photopeak to its appropriate energy. This is accomplished by counting a series of known radionuclides (energies) to determine their channel positions on the energy spectrum. The efficiency calibration is required to relate measured counts to the absolute values of the sample activities and it depends on kind and size of the detector, instrument settings, sample geometry (i.e., the size and shape of the container), sample volume, and shielding (background activities). Consequently, it is necessary to calibrate the energy and efficiency of each machine for every amplifier setting and sample geometry that will be used. Typical efficiencies for the low energy ^{210}Pb photopeak (46.52 keV) are ~0.5% and the efficiencies are about a factor of 3–5 less at the higher energies of ^{7}Be (477.59 keV) and ^{137}Cs (661.66 keV). Because of these low efficiencies and the low activities in most samples (some Chernobyl samples are an exception) counting times of about 1 day are needed to obtain enough counts to reduce the counting error to $<$10%. Typical self-absorption correction factors (Cutshall et al. 1983) at the low energy of ^{210}Pb can range from 10 to 80% depending on the size and shape of the sample while the self-absorption correction factor at the higher energy of ^{137}Cs is negligible.

Determining the efficiency requires the use of a standard for which the activity is known. Unfortunately there are no commercially available standards of soils or sediments that are suitable for the efficiency determination of the entire suite of radionuclides commonly measured (^{210}Pb, ^{7}Be, ^{137}Cs, ^{40}K) although there are a couple of samples that can be used as Quality Assurance samples or as a laboratory standard for efficiency calibration for ^{137}Cs, such as NIST 4350B Columbia River Sediment and International Atomic Energy Agency Reference Material IAEA-375. A list of primary standards available for the

calibration of instruments and chemical procedures is given in Baskaran et al. (2009). In particular, RGU-1 (IAEA – 400 μg g^{-1} with ^{238}U concentration with all its daughter products in secular equilibrium) is a suitable standard for the calibration of ^{210}Pb. Alternatively, it is possible to prepare a standard by spiking a "clean" soil or sediment with the appropriate radionuclides of known activities (for example, Amersham plc QCY44 or NG4 Mixed Radionuclide Solutions) and then placing those prepared soils in the appropriate container for the efficiency calibration of that geometry.

25.4 Methods for Calculating Soil Erosion

Soil erosion can be calculated by the change in the inventory of radionuclides. While the same basic approaches can be used with any of the radionuclides, we detail the use of ^{137}Cs in erosion studies because it was for ^{137}Cs that the methods were originally developed.

Estimation of the erosion rate using ^{137}Cs inventories is typically addressed as an inverse problem with known ^{137}Cs inventories, cultivation and precipitation histories. The simplest method to estimate erosion rates is by a comparison of the ^{137}Cs inventory in soil cores with a reference value from a nearby non-eroded site. The non-eroded site represents the expected baseline fallout to the local geographic area, so that an eroded site would be expected to have less inventory compared to the non-eroded site. Various models have been applied to ^{137}Cs inventories where the erosion rate is assumed to be correlated to the percent of the ^{137}Cs inventory lost from a site (Ritchie et al. 1974; Spomer et al. 1985; Brown et al. 1981; Kachanoski and deJong 1984; DeJong et al. 1986; Lowrance et al. 1988; Soileau et al. 1990; Montgomery et al. 1997; Walling et al. 1999a, b; Fornes et al. 2005). These methods have been recently reviewed (Walling et al. 2002; Poreba 2006) in more detail than we present below and an analysis of these methods led Zapata et al. (2002) to conclude that there are uncertainties associated with the model selection used to estimate erosion rates, that most of the models do not address short-term changes in erosion rates such as those related to changes in land use and management practices, and that the methodology needs further standardization of the protocols for its general application worldwide.

25.4.1 Empirical, Non-Linear Model

Studies conducted in the 1960s and early 1970s in which ^{137}Cs inventory loss was compared with soil loss estimated using the Universal Soil Loss Equation (Wischmeier and Smith 1978) showed a strong, non-linear empirical relationship at several sites following the equation

$$E = 0.0087P^{1.18} \tag{25.1}$$

where E is erosion rate (g cm^{-2} $year^{-1}$) and P is the percent ^{137}Cs inventory lost from the study site (Ritchie et al. 1974). Percent radionuclide inventory lost is defined as

$$P = (I_{ref} - I_{site})/I_{ref}{}^{*}100 \tag{25.2}$$

where I_{ref} is the ^{137}Cs inventory from an undisturbed reference site (Bq m^{-2}) and I_{site} is the ^{137}Cs inventory for the study site. This led to the development of a number of models to calculate erosion rate on the basis of percent inventory lost. In essence, the model assumes a uniform distribution of ^{137}Cs throughout the soil profile so that erosion removes a proportional fraction of the inventory. This approach can result in significant error in the estimation of erosion rate in areas where land use, conservation practices, precipitation or other environmental conditions are not constant throughout the sampling period. For example, if atmospheric ^{137}Cs fallout were confined to the upper layer of soil prior to being eroded or distributed within the cultivation layer, a singular erosion event occurring just after the atmospheric fallout peak in 1964 (following the peak in stratospheric fallout) or in 1986 (following Chernobyl fallout in Europe) would remove a disproportionate amount of ^{137}Cs inventory and result in an overestimate of the soil erosion rate throughout the sampling period. Conversely, a major erosion event today will remove only a small fraction of the inventory because of the downward migration of ^{137}Cs in the

intervening time period and may result in an underestimate of the erosion rate. The use of a reference site does not solve this problem.

25.4.2 Linear Box Model Methods

There are two major classes of models that linearly correlate the percent ^{137}Cs inventory lost with erosion rate. One approach assumes that the total ^{137}Cs inventory is eligible for erosion (Linear 1-Box model; Brown et al. 1981; Spomer et al. 1985) and those in which only the ^{137}Cs inventory within a surface or tillage layer is eligible for erosion (Linear-2Box model; DeJong et al. 1986; Lowrance et al. 1988; Soileau et al. 1990; Montgomery et al. 1997). The key difference between the Linear-1Box and Linear-2Box models lies in the vertical distribution of ^{137}Cs. The Linear-1Box model assumes (sometimes incorrectly) that the entire ^{137}Cs inventory is confined to the tillage layer, whereas the Linear-2Box model allows for some portion of the inventory to reside beneath the tillage layer where it is unavailable for erosion. Spomer et al. (1985) used the Linear-1Box model to describe soil erosion during the period 1954–1974, so that

$$E = DP_L K/T \tag{25.3}$$

where D is the average tillage mixing depth (cm), K is the dry bulk density of the soil (g cm^{-3}), and T is the time since the onset of ^{137}Cs deposition (y). P_L is defined as

$$P_L = (I_{ref} - I_{site})/I_{ref} \tag{25.4}$$

The Linear-2Box model (i.e., tillage depth $<$ ^{137}Cs penetration depth) described soil erosion with the relationship

$$E = DP_{till} K/T \tag{25.5}$$

P_{till} is analogous to P_L, but the inventory is confined to the tillage layer or to the same depth as the tillage layer at reference sites. Comparisons of results obtained with both the Linear 1-Box and Linear 2-box models indicate little differences in derived erosion rates at Spomer et al.'s (1985) field site (Fornes et al. 2005).

25.4.3 Time-Dependent Model Methods

Some approaches (detailed in Ritchie et al. 1974) are limited in their use because the relationship between erosion rate and ^{137}Cs inventory is incorrectly assumed to be independent of time or cultivation, even failing to account for the radioactive decay of ^{137}Cs (Kachanoski and deJong 1984). These various approaches produced a wide range of erosion rates at a single site (Fornes et al. 2000) confirming that model assumptions significantly influence ^{137}Cs-derived soil erosion rates. Thus, these models are limited because they are single time-step models that do not consider the time-dependent nature of ^{137}Cs fallout (Kachanoski and deJong 1984; Spomer et al. 1985; Walling et al. 1999a, b) or the downcore migration of ^{137}Cs (Figs. 25.9–25.11).

It is possible to obtain improved estimates of soil erosion rates based upon changes in ^{137}Cs inventories by addressing issues associated with model assumptions and changes in soil conservation practices by modeling the time-dependent ^{137}Cs fallout, precipitation and soil cultivation (Kachanoski and deJong 1984; Walling and He 1997a, b; Zhang et al. 1999; Fornes et al. 2005). Using this approach, the equation describing the rate of change of total ^{137}Cs inventory is

$$\partial I/\partial t = F(t) - EC(t) - \lambda I \tag{25.6}$$

where I is ^{137}Cs inventory (Bq cm^{-2}), E is erosion rate (g cm^{-2} year^{-1}), C(t) is the concentration of ^{137}Cs (Bq g^{-1}), F(t) is the time-dependent atmospheric fallout of ^{137}Cs (Bq cm^{-2}), and λ is the radioactive decay constant (year^{-1}). Temporal variation of ^{137}Cs fallout, F(t), can be derived from the measured fallout data (Fig. 25.3) with the magnitude adjusted to the local ^{137}Cs reference inventory (Health and Safety Laboratory 1977; Cambray et al. 1989). This model can be kept compatible with the Linear-1Box and Linear-2Box models, by assuming steady-state erosion and cultivation. Soil erosion rates can also be calculated under more detailed constraints such as precipitation-dependent erosion and ephemeral homogenization of the cultivated layer (Walling and He 1997a, b; Zhang et al. 1999; Fornes et al. 2005) for more accurate and realistic erosion rates.

Figure 25.13 illustrates the differences in calculated erosion rates that model assumptions governing the

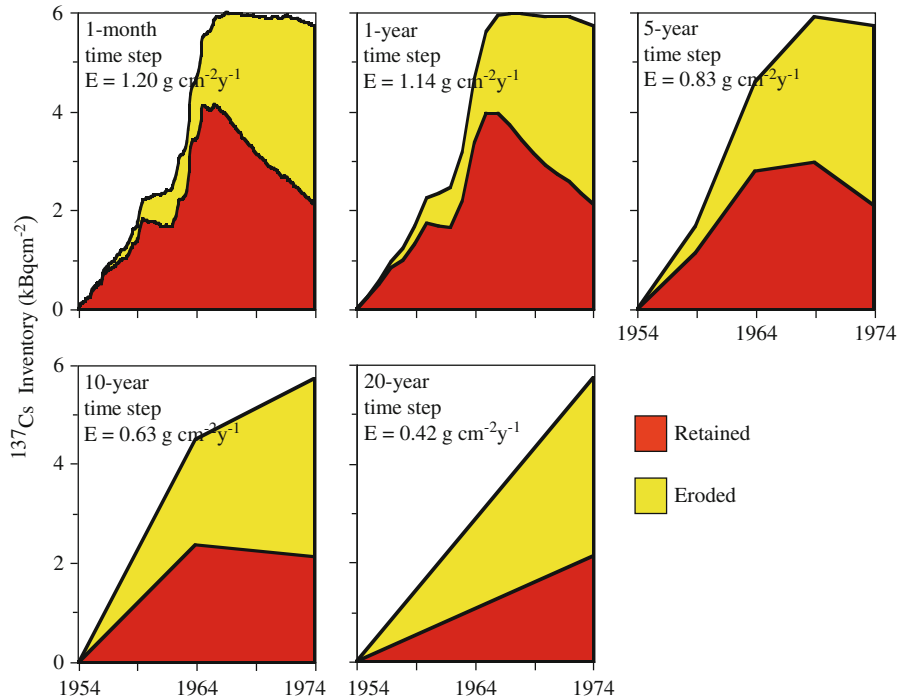

Fig. 25.13 Calculated ^{137}Cs inventories in a soil subject to atmospheric deposition of ^{137}Cs, periodic (annual) cultivation, and erosion over the time period 1954–1974. Note that inclusion of monthly data results in an erosion rate about 3 times larger than that calculated from the soil inventory only at the end of the 20-year time period. After Fornes et al. (2005)

choice of time step exert on the calculated erosion rates. In these simulations of Fornes et al. (2005), the erosion rate decreased by a factor of three as the model time step was increased from 1 month to 20 years. With a single 20-year time step, erosion rates are virtually the same as those estimated by Spomer et al. (1985) because Spomer et al. (1985) used a Linear-1Box model to describe soil erosion during a single time interval of 1954–1974. The modest differences between the 20-year time step and those reported by Spomer et al. (1985) can be explained by noting that the cultivation depth used in the Fornes et al. (2005) simulations was 10 cm, but Spomer et al. (1985) used a 15 cm cultivation depth. Deposition, cultivation, and erosion in the Spomer et al. (1985) model occur in a single step beginning c. 1954 and ending when the core was collected in 1974. The Fornes et al. (2005) model incorporates a monthly time step (Fig. 25.13) so the 20-year interval is approximated by 240 monthly time steps of deposition and erosion. These results indicate that ^{137}Cs-derived erosion rates are highly sensitive to the length of the time step used in the model because of the combination of the timing of the fallout, cultivation, and erosion. These results suggest that models that fail to account for temporal variations in atmospheric deposition and/or cultivation practices can grossly miscalculate erosion rates.

25.4.4 Tillage Erosion

While the radionuclide inventory in a core and/or the downcore profile of a radionuclide in that core may indicate erosion, the models described above do not necessarily inform the cause of that erosion. The pattern of radionuclide inventories in a field may be strongly influenced by tillage translocation rather than water erosion. For example, poor agreement has been reported between spatially-distributed ^{137}Cs -derived soil redistribution rates with those derived from water erosion (Quine 1999). Reduced inventories on hillslope convexities and deposition in hollows have been attributed to soil loss caused by tillage redistribution rather than by water erosion

(DeJong et al. 1983; Lobb et al. 1995). Consequently, several workers have developed models which attempt to distinguish the two drivers of radionuclide redistribution and thereby obtain an estimate of the erosion caused solely by water erosion (Govers et al. 1994, 1996; Lobb and Kachanoski 1999). Van Oost et al. (2006) provide a review of the literature on tillage erosion and conclude that based on a global data set tillage erosion rates are comparable to or higher than water erosion rates. They note that because of the widespread use of tillage practices, the high translocation rates resulting from tillage, and the effects of tillage on soil properties, that tillage erosion should be considered in soil landscape studies.

The most widespread used tillage model treats tillage erosion as a diffusion-type process (Govers et al. 1994). The model of Govers et al. (1994) relates the rate of soil translocation to the soil bulk density, the average soil translocation distance in the direction of tillage, and the depth of tillage. They treat translocation distances resulting from a single tillage pass to be linearly and inversely related to slope and that multiple passes in opposing directions results in a net downslope transport. Additional assumptions are that the tillage depth and soil bulk density do not vary in space, tillage soil translocation can be expressed as a linear function of the slope gradient, and tillage is conducted in opposing directions. Using the continuity equation they determine that the tillage erosion may be written as

$$E = -\frac{\partial Q_s}{\partial x} = -D\rho_b b\frac{\partial h}{\partial x} = k_{til}\frac{\delta^2 h}{\delta x^2} \qquad (25.7)$$

where E is the tillage erosion rate (kg m^{-2} a^{-1}); Q_s is the rate of soil translocation in the direction of tillage (kg m^{-1} a^{-1}); D is the tillage depth (m); ρ_b is the soil bulk density (kg m^{-3}); x is the distance (positive downslope) (m); d is the average soil translocation distance in the direction of tillage (m a^{-1}) (=a + bS where a and b are regression constants (m a^{-1}) and S is the slope tangent (positive upslope; negative downslope) (dimensionless)); h is the height at a given point of the hillslope (m); and k_{til} (=$-D\rho_b b$) is the tillage transport coefficient (kg m^{-2} a^{-1}).

This model has been applied to a number of studies to compare different plowing directions (Van Muysen et al. 2002; St Gerontidis et al. 2001; De Alba 2001; Quine and Zhang 2004; Heckrath et al. 2006), and erodability of the landscape (Lobb et al. 1999) as affected by implement characteristics (tool shape, width, length) and operational parameters (tillage depth, speed, tillage direction). Reported implement erosivities as characterized by the tillage transport coefficient are fairly consistent and range from 400 to 800 kg m^{-2} $year^{-1}$ for mechanized plowing and from 70 to 260 kg m^{-2} $year^{-1}$ for non-mechanized agriculture (Van Oost et al. 2006). Van Oost et al. (2006) also report that decreasing tillage depth and plowing along contour lines substantially reduce tillage erosion rates and can be considered as effective soil conservation strategies.

25.4.5 Wind Erosion

Compared to water there has been relatively little work using ^{137}Cs to study aeolian processes of erosion and deposition. Recently, however, the application of ^{137}Cs to study wind erosion has received some attention (Sutherland and deJong 1990; Sutherland et al. 1991; Chappell 1996, 1998; Yan and Zhang 1998; Yan et al. 2001; Yan and Shi 2004; Hu et al. 2005). The determination of the wind erosion rate is important in assessing the extent and intensity of desertification and the effectiveness of counter-measures.

Calculation of wind erosion rates has been based on the same proportional inventory models that are sometimes used to estimate erosion by water (Sutherland and deJong 1990; Walling and Quine 1993), although it is recognized that these models sometimes suffer from the same issues affecting their use to quantify water erosion – failure to account for surface enrichment of ^{137}Cs and ^{137}Cs dilution by tillage. Mass balance models (Kachanoski and deJong 1984; Zhang et al. 1990) are more suitable for assessing soil erosion in soils where ^{137}Cs is distributed uniformly, such as croplands. In settings where the ^{137}Cs profile is not homogeneous, such as grasslands, the profile distribution model is more appropriate. The calculation of wind erosion loss in these models (Yan et al. 2001; Hu et al. 2005) is estimated by

$$E = CPR * Bd * DI * 10^4/T \qquad (25.8)$$

where E is the net wind erosion rate of the sample site (Mg ha^{-1} a^{-1}); Bd is the bulk density of the soil (Mg m^{-3}); DI is the sampling depth increment (assumed = plow depth in farmlands, Sutherland and deJong 1990; Walling and Quine 1993) and in undisturbed soils it is approximately the depth over which ^{137}Cs is found (~0.1–0.3 m); T is the time period between the year of initial ^{137}Cs fallout (assumed to be the year of maximum fallout, 1963) and the sampling year of the study; CPR is the percentage residual at a sampling point in the field relative to the native control area (%):

$$\mathrm{CPR} = (\mathrm{CPI} - \mathrm{k} * \mathrm{CRI}) * 100/(\mathrm{k} * \mathrm{CRI}) \quad (25.9)$$

where CPI is the ^{137}Cs inventory at the sampling site (Bq m^{-2}); k is a coefficient of ^{137}Cs redistribution caused by snow-blown and vegetation removal (sometimes set =1; =0.95 in Yan et al. 2001); and CRI is the ^{137}Cs inventory at the reference site (Bq m^{-2}).

Studies using this model to quantify wind erosion yield rates that range from 300 to 8,400 Mg m^{-2} a^{-1} depending on the vegetative cover (Yan et al. 2001; Yan and Shi 2004; Hu et al. 2005) where grasslands exhibit the least erosional loss and croplands and dunelands the highest. In one study (Li et al. 2005), an attempt was made to estimate the relative magnitudes of both wind and water erosion in the same study area, and the authors report that wind erosion can account for at least 18% of the total soil loss.

25.5 Recent Applications

In this section, we describe new applications of ^{137}Cs and other radionuclides in studies of surface erosion and deposition.

25.5.1 Single Event Erosion Measurement

One limitation of the longer-lived radionuclides ^{137}Cs and ^{210}Pb is their inability to quantify erosion over short time periods; for instance, the erosion occurring during a single storm. ^{137}Cs and ^{210}Pb are unsuitable for such studies because the change in inventory due to erosion during a single event is small compared to the total inventory. Walling and Quine (1990) estimated that at least a decade of erosion is necessary to produce a large enough change in ^{137}Cs inventory ($t_{1/2}$ = 30.1 years) that the difference is measurable. Following this reasoning, at least 5–8 years of erosion would be required to recognize erosion using changes in $^{210}Pb_{xs}$ inventory ($t_{1/2}$ = 22.3 years). ^{7}Be has a sufficiently short halflife ($t_{1/2}$ = 53 days) that Blake et al. (1999), Walling et al. (1999a, b) and Wilson et al. (2003) used the radionuclide to estimate erosion occurring during single rainfall events. The workers determined the pre-storm and post-storm inventory of ^{7}Be as well as the delivery with precipitation. The erosion during the single event studied by Wilson et al. (2003) corresponded to 23% of the average annual erosion rate determined by ^{137}Cs and the mass-balance approach yielded an erosion amount that matched the erosion determined from sediment flux off the field.

Vitko (2007) used ^{7}Be to recognize redistribution of plowed soil from ridges into adjacent furrows finding that fields plowed along contour had greater retention of ^{7}Be than fields plowed up-down the slope presumably due to less soil erosion and/or greater deposition.

25.5.2 Sediment Sources

The radionuclides ^{7}Be, ^{137}Cs, and ^{210}Pb have been used individually and in tandem to quantify the relative contributions of different processes of erosion to sediment. Nagle et al. (2007) used the activity of ^{137}Cs in suspended sediments to determine the provenance of sediment. Collins and Walling (2007) utilized ^{137}Cs and several other constituents in a multivariate sediment mixing model to identify principle sources of fine sediment. He and Owens (1995) used ^{137}Cs, $^{210}Pb_{xs}$, and ^{226}Ra in tandem to provide radionuclide fingerprints of cultivated land, uncultivated land, and stream banks and their contributions to the sediment pool. Walling and Woodward (1992) used ^{7}Be, ^{137}Cs, $^{210}Pb_{xs}$ to distinguish sediment from surficial and channel sources and the trend in ^{7}Be during the studied event allowed them to recognize changing sources. Brigham et al. (2001) used $^{210}Pb_{xs}$, ^{7}Be, and ^{137}Cs as separate tracers to determine the relative importance of surficial and streambank erosion. There was

substantial variation in the estimated percentage of sediment from surface soil erosion – $^{137}Cs = 34\%$, $^{210}Pb_{xs} = 71\%$, $^{7}Be = 91\%$. Gellis and Landwehr (2006) used ^{137}Cs and unsupported ^{210}Pb, stable isotopes (del ^{13}C and del ^{15}N), total carbon, nitrogen, and phosphorus to successfully partition sources of fine-grained suspended sediment in the Pocomoke River watershed from cropland, forest, channel and ditch banks, and ditch beds. Devereux et al. (2010) used concentrations of 63 elements and two radionuclides to fingerprint fine sediment sources by both physiographic province (Piedmont and Coastal Plain) and source locale (streambanks, upland and street residue).

Here we consider several specific examples of the use of tracers in source identification. Whiting et al. (2005) established the contribution of streambanks to the suspended sediment flux with a two-component mixing model that used the distinctive radionuclide signatures of the streambanks and of the landscape soils to define the end members of the mixing model (Fig. 25.14). Sediment delivered to the channel by erosion of the soil surface has relatively high activities of ^{7}Be and ^{210}Pb because of the atmospheric delivery of the radionuclides to the soil surface (Fig. 25.12). Sediment delivered to the channel by bank erosion (largely toppling) has much lower radionuclide activities because the low-activity material from deeper in the bank dilutes the high activity material from atop the bank. The height of the collapsed bank is so much larger than the depth of penetration of ^{7}Be into the soil that the activity of ^{7}Be in the eroded bank material is effectively zero. The depth to which the bank material is removed corresponds to that part of the soil profile where only the low-activity supported ^{210}Pb is found. Consequently, the ^{210}Pb activity of the bank material is much lower than the surface activity and is similar to the constant value that reflects in situ decay of soil minerals.

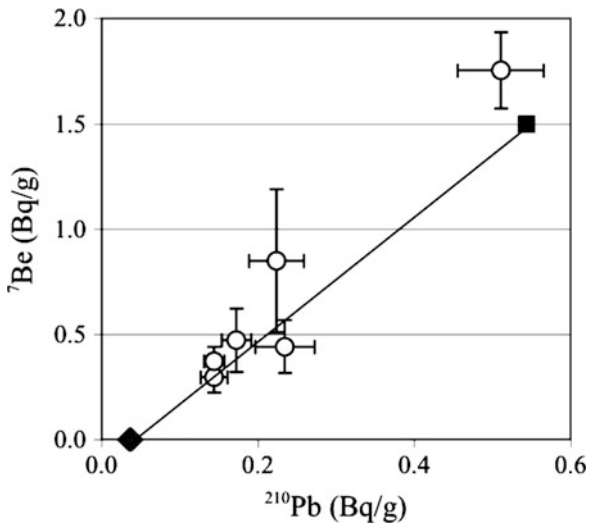

Fig. 25.14 The suspended sediment samples (o) along Soda Butte Creek in Yellowstone National Park, Wyoming, USA, are intermediate between two endmember sources for fine sediment: bank material (*diamond*) and surficial soils (*square*)

In another study, Whiting et al. (2001) used the distinct distribution of ^{7}Be, ^{137}Cs, and ^{210}Pb with depth in soils on an agricultural plot (Fig. 25.12) and the measured radionuclide flux in runoff in multiple mass balances to quantitatively estimate the areal extent of rill and sheet erosion and the characteristic depth of erosion associated with each mechanism. They examined 15.5 million possible combinations of the depth and areal extent of rill and sheet erosion and found that the best solution to the mass balances corresponded to rills eroding 0.38% of the basin to a depth of 35 mm and sheetwash eroding 37% of the basin to a depth of 0.012 mm. Rill erosion produced 29 times more sediment than sheet erosion.

The identification of sources and depositional locations identified by the radionuclide ratios as discussed herein can be the basis for quantifying a sediment budget. Blake et al. (2002) used ^{7}Be and ^{137}Cs to quantify various elements of a sediment budget – soil erosion and remobilization from hillslopes, erosion and deposition in river channels, and floodplain deposition. ^{137}Cs has been a common tool for characterizing soil redistribution on landscapes (Walling and Quine 1992; Owens et al. 1997; Walling et al. 2003; Kaste et al. 2006).

25.5.3 Pu as a Tracer

$^{239,240}Pu$ may be a promising substitute for ^{137}Cs measurements. Stratospheric $^{239,240}Pu$ is also bomb-derived, behaves similarly once delivered to the earth surface, and gives equivalent information. In fact, Figs. 25.11 and 25.15 show how similar the profiles for the two radionuclides can be and Fig. 25.16 illustrates the strong correlation between ^{137}Cs and $^{239,240}Pu$ inventories. There are several reasons why $^{239,240}Pu$ may become used more often than ^{137}Cs. With the development of a method for using inductively coupled plasma mass spectrometry (ICPMS)

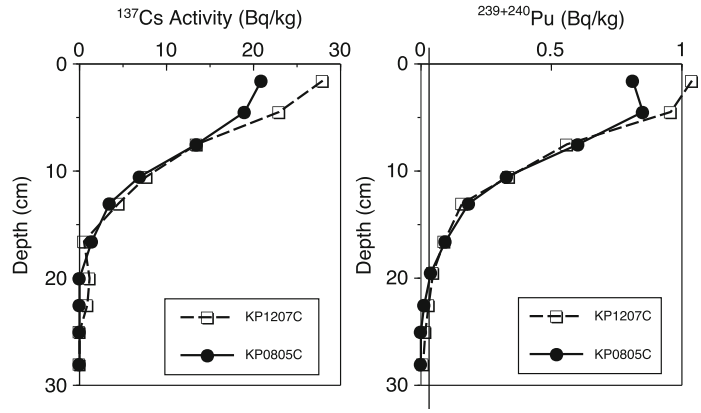

Fig. 25.15 Comparison of ^{137}Cs and $^{239+240}$Pu profiles in undisturbed prairie soils from Konza Prairie, KS. Plutonium data courtesy of Michael Ketterer

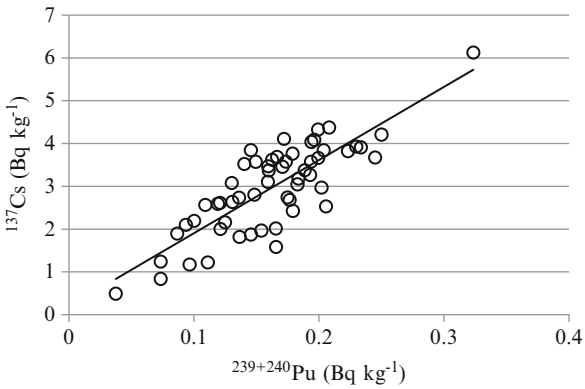

Fig. 25.16 ^{137}Cs inventory vs. ^{239,240}Pu inventory for soil auger samples from 54 sites in the Murder Creek, Georgia USA watershed (from Stubblefield et al. ms)

and high sample through-put, the use of ^{239,240}Pu may be more cost effective (Ketterer and Szechenyi 2008). Moreover, ^{137}Cs half-life ($t_{1/2}$ = 30.1 years) is such that peak inventories were observed in the mid- to late-1960s, and by 2010 inventories are only ~40% of original values and dropping. The halflife of both Pu isotopes is several thousand years. Finally, the ^{240}Pu/^{239}Pu values in fallout in the 1950s and after 1965 differ which may allow partial differentiation of the time frame of erosion.

25.5.4 Use with Other Techniques and in Other Settings

Recently we have seen the use of the fallout radionuclides in conjunction with other erosion measurement techniques. Fondran (2007) combined the use of multiple mass-balances of radionuclides and a laser line scanner with sub-millimeter vertical resolution. With the laser line scanner, Lorimor was able to measure changes in topography (erosion and deposition) and compare these results to the estimates of the depth and areal extent of rills and sheetwash as determined from the multiple mass balances. In the same study, rare earth element tagged soils were deployed to provide information on the proportion of sediment delivered from the top of the slope compared to the middle and bottom of the slope (Stubblefield et al. 2006). O'Farrell et al. (2007) used pond sediment volumes, ^{137}Cs and ^{210}Pb activities, and ^{10}Be and ^{26}Al activities to examine different approaches and timeframes for estimating landscape denudation. Walling et al. (1999a, b) used ^{7}Be and ^{137}Cs respectively to evaluate event and decadal erosion rates. The conjunctive use of fallout radionuclides (Mabit et al. 2008) especially with other radionuclides, promises to provide key information on variation in denudation rates over time driven by changes in climate and landuse.

Yet other applications include using radionuclide based sedimentation estimates to test predictions of floodplain sedimentation (Siggars et al. 1999) and to compare aerial photography-derived and radionuclide-derived meander migration rates (Black et al. 2010) or accretion rates (Provansal et al. 2010). Various workers have used ^{7}Be and/or ^{210}Pb to investigate resuspension in rivers and estuaries (Fitzgerald et al. 2001; Wilson et al. 2003, 2005, 2007; Jweda et al. 2008), erosion after forest harvesting (Schuller et al. 2006), and wildfire (Blake et al. 2009).

While the use of radionuclides in surficial studies has focused on tracing fine materials, Salant et al. (2006) used ^{7}Be to recognize and track medium and coarse sand released from an impoundment. Fisher et al. (2010) likewise used ^{7}Be to constrain the timescales of sediment storage associated with large woody debris.

25.6 Future Directions

Although there are about 5,000 papers in the literature devoted to the radionuclides discussed in this chapter there is still room for improvement in the methodologies and applications. From a technological perspective, improvements in instrumentation and detection and lowering of costs should enable greater numbers of samples to be collected and analyzed. For example, the development of larger, low cost gamma detectors that do not require liquid nitrogen cooling will enable a more routine use of the equipment, field deployment and more detailed spatial resolution. This could lead to watershed scale or even landscape scale studies. Another technological improvement could be the development of ICP-MS methods for the measurement of ^{137}Cs and ^{210}Pb. Measurement of gamma decays is inefficient because it measures only those atoms that undergo decay during the counting period. But the vast majority of the atoms of interest do not undergo decay during the counting period, especially for the longer lived isotopes. Instead, mass measurements have the advantage of measuring all the atoms that are present in the sample. While ICP-MS methods have been developed for Pu isotopes (Ketterer et al. 2002) it appears that natural levels of ^{137}Cs and ^{210}Pb cannot be detected by current instrumentation. However, with improvements in ICP-MS technology this may change and permit cost-effective analyses of much larger numbers of samples. As with the development of larger low cost gamma detectors, the development of these techniques could enable much higher spatial resolution studies. For example studies comparing ^{239,240}Pu-derived erosion rates as a surrogate for ^{137}Cs-derived erosion rates can be done now, since there are already ICP-MS methods for ^{239,240}Pu and larger numbers of samples can be run for ^{239,240}Pu than for ^{137}Cs.

Earlier in this chapter we demonstrated that the derived erosion rate is model dependent, and in particular, also depends on the time interval used to evaluate erosion. But these models do not account for the steady, downward migration of the radionuclides. Further progress will require the incorporation of the downward migration into the time dependent erosion models. Furthermore, these models will need to be more comprehensive in their treatment of the downward migration process. Particle mixing by bioturbation as well as solute transport with adsorption will both need to be included in models to enable a better description of the vertical profiles as a function of time. Furthermore, there is evidence that the downward migration process is not steady, and may be affected by non-linear adsorption and/or flow through macropores or channels. A more rigorous evaluation and treatment of these processes needs investigation and incorporation into the models.

It may be possible to use the much better ^{137}Cs soil data sets collected following Chernobyl than the older soil profiles collected a couple of decades after stratospheric fallout to constrain erosion models, quantify soil properties, and improve estimates of soil transport and sources. Even more intriguing is the possibility of combining from the same soil column ^{137}Cs profiles that are dominated by Chernobyl fallout with ^{239,240}Pu profiles derived from global fallout because this will enable comparison of two different tracers over two different time periods within the same soil profile. Furthermore, it may be possible to find locations where the ^{137}Cs signal from stratospheric fallout is comparable in magnitude to the ^{137}Cs fallout from Chernobyl. In such a situation it may be possible to identify and separate the two overlapping signals which will help constrain soil processes and model coefficients.

Finally, soil fertility and C sequestration in soils remain global issues. Thus, accurately determining soil erosion rates, which clearly impacts soil fertility and affects estimates of C sequestration and C removal, remains an important component in research on these topics. Similar studies could also be done to relate past and current erosion rates to land usage to provide both estimates of the historical impacts of land usage on erosion and also future impacts of land usage on C storage and cycling.

Acknowledgements This chapter is dedicated to the memory of Jerry Ritchie.

We would like to thank our former students for their contributions to our research, some of which is highlighted in this chapter: undergraduates Rita Cabral, Joel Saylor, Derek Smith,

Natalie Vajda, and Lauren Vitko; graduate students Chris Bonniwell, Travis Bukach, Carol Fondran, and Chris Wilson; post-doctoral research associates Bill Fornes and Andrew Stubblefield; and colleagues Michael Ketterer, J. Wojciech Mietelski, Klas Rosén, Fred Soster, Louis Thibodeaux, and their students. James Kaste and an anonymous reviewer provided comments that improved the manuscript.

References

Aoyama M, Hirose K, Igarashi Y (2006) Re-construction and updating our understanding on the global weapons tests ^{137}Cs fallout. J Environ Monitor 8:431–438

Ayub JJ, Di Gregorio DE, Velasco H, Huck H, Rizzotto LF (2009) Short-term seasonal variability in Be-7 wet deposition in a semiarid ecosystem of central Argentina. J Environ Radioact 100:977–981

Azahra M, Camacho-Garcia A, Gonzalez-Gomez C, Lopez-Penalver JJ, El Bardouni T (2003) Seasonal Be-7 concentrations in near-surface air of Granada (Spain) in the period 1993–2001. Appl Radiat Isot 59:159–164

Balistrieri LS, Murray JW (1984) Marine scavenging: trace metal adsorption by interfacial sediment from MANOP site H1. Geochim Cosmochim Acta 48:921–929

Baskaran M (1995) A search for the seasonal variability on the depositional fluxes of ^{7}Be and ^{210}Pb. J Geophys Res 100:2833–2840

Baskaran M (2011) Po-210 and Pb-210 as atmospheric tracers and global atmospheric Pb-210 fallout: a review. J Environ Radioact 102:500–513

Baskaran M, Santschi PH (1993) The role of particles and colloids in the transport of radionuclides in coastal environments of Texas. Mar Chem 43:95–114

Baskaran M, Coleman CH, Santschi PH (1993) Atmospheric depositional fluxes of Be-7 and Pb-210 at Galveston and College Station, Texas. J Geophys Res 98:20555–20571

Baskaran M, Ravichandran M, Bianchi TS (1997) Cycling of ^{7}Be and ^{210}Pb in a high DOC, shallow, turbid estuary of southeast Texas. Estuar Coast Shelf Sci 45:165–176

Baskaran M, Hong G-H, Santschi PH (2009) Radionuclide analysis is seawater. In: Wurl O (ed) Practical guidelines for the analysis of seawater. CRC Press, Boca Raton, pp 259–304

Beck HL (1999) External radiation exposure to the population of the continental U.S. from Nevada weapons tests and estimates of deposition density of radionuclides that could significantly contribute to internal radiation exposure via ingestion. Report to the National Cancer Institute, P.O. #263-MQ-909853. New York

Black E, Renshaw CE, Magilligan FJ, Kaste JM, Dade WB, Landis JD (2010) Determining lateral migration rates using fallout radionuclides. Geomorphology 123:364–369

Blake WH, Walling DE, He Q (1999) Fallout beryllium-7 as a tracer in soil erosion investigations. Appl Radiat Isot 51:599–605

Blake WH, Walling DE, He Q (2002) Using cosmogenic Beryllium-7 as a tracer in sediment budget investigations. Geogr Ann 84:89–102

Blake WH, Wallbink PJ, Wilkinson SN, Humphreys GS, Doerr SH, Shakesby RA, Tomkins KM (2009) Deriving hillslope sediment budgets in wildfire affected forests using fallout radionuclide tracers. Geomorphology 104:105–116

Bonniwell EC, Matisoff G, Whiting PJ (1999) Fine sediment residence times in rivers determined using fallout radionuclides (^{7}Be, ^{137}Cs, ^{210}Pb). Geomorphology 27:75–92

Bossew P, Kirchner G (2004) Modeling the vertical distribution of radionuclides in soil. Part 1. The convection-dispersion equation revisited. J Environ Radioact 73:127–150

Boudreau BP (1986a) Mathematics of tracer mixing in sediments: I. Spatially-dependent, diffusive mixing. Am J Sci 286:161–198

Boudreau BP (1986b) Mathematics of tracer mixing in sediments: II. Nonlocal mixing and biological conveyor-belt phenomena. Am J Sci 286:199–238

Brigham ME, McCullough CJ, Wilkinson P (2001) Analysis of suspended-sediment concentrations and radioisotope levels in the Wild Rice River basin, northwestern Minnesota, 1973–98. US Geological Survey Water Resources Investigation Report 2001-4192

Brown RB, Kling GF, Cutshall NH (1981) Agricultural erosion indicated by ^{137}Cs redistribution: II. Estimates of erosion rates. Soil Sci Soc Am J 45:1191–1197

Brudecki K, Suwaj J, Mietelski JW (2009) Plutonium and ^{137}Cs in forest litter: the approximate map of plutonium from Chernobyl deposition in Northeastern and Eastern Poland. Nukleonika 54(3):199–209

Bundt M, Albrecht A, Froidevaux BP, Fluhler H (2000) Impact of preferential flow on radionuclide distribution in soil. Environ Sci Technol 34:3895–3899

Caillet S, Arpagaus P, Monna F, Dominik J (2001) Factors controlling Be-7 and Pb-210 atmospheric deposition as revealed by sampling individual rain events in the region of Geneva, Switzerland. J Environ Radioact 53:241–256

Callender E, Robbins JA (1993) Transport and accumulation of radionuclides and stable elements in a Missouri River reservoir. Water Resour Res 29:1787–1804

Cambray RS, Playford K, Lewis GNJ (1985) Radioactive fallout in air and rain: results to the end of 1984. In: Report *AERE-R11915*, Harwell

Cambray RS, Playford K, Carpenter RC (1989) Radioactive fallout in air and rain: results to the end of 1988. Report no. AERE-R 10155, U.K. Atomic Energy Authority

CDC (2006) Report on the feasibility of a study of the health consequences to the American population from nuclear weapons tests conducted by the United States and Other Nations. http://www.cdc.gov/nceh/radiation/fallout/. Accessed date: March 17, 2010

Chappell A (1996) Modelling the spatial variation of processes in redistribution of soil: digital models and ^{137}Cs in the south-west Niger. Geomorphology 17:249–261

Chappell A (1998) Using remote sensing and geostatistics to map ^{137}Cs-derived net soil flux in the south-west Niger. J Arid Environ 39:441–455

Chen G, Flury M, Harsh JB, Lichtner PC (2005) Colloid-facilitated transport of cesium in variably saturated Hanford sediments. Environ Sci Technol 39:3435–3442

Ciffroy P, Reyss J, Siclet F (2003) Determination of the residence time of suspended particles in the turbidity maximum

of the Loire estuary by ^{7}Be analysis. Estuar Coast Shelf Sci 57:553–568

Collins AL, Walling DE (2007) The storage and provenance of fine sediment on the channel bed of two contrasting lowland permeable catchments, UK. River Res Appl 23: 429–450

Collins AL, Walling DE, Sichingabula HM, Leeks GJL (2001) Using 137Cs measurements to quantify soil erosion and redistribution rates for areas under different land use in the Upper Kaleya River basin, southern Zambia. Geoderma 104:229–323

Coughtrey PJ, Thorne MC (1983) Radionuclide distribution and transport in terrestrial and aquatic ecosystems: a critical review. A.A. Balkema, Rotterdam

Cremers AE, De Preter P, Maes A (1988) Quantitative analysis of radiocaesium retention in soils. Nature 335:247–249

Cutshall NH, Larsen IL, Olsen CR (1983) Direct analysis of ^{210}Pb in sediment samples; self adsorption correction. Nucl Instr Meth 206:309–312

Darwin C (1881) The formation of vegetable mould through the action of worms. London: J. Murray (Facsimilies republished in 1982 and 1985, University of Chicago Press, Chicago)

Davis L (1986) Concern over Chernobyl-tainted birds. Sci News 130:54

de Alba S (2001) Modeling the effects of complex topography and patterns of tillage on soil translocation by tillage with mouldboard plough. J Soil Water Conserv 56:335–345

De Cort M, Dubois G, Fridman SD, Germenchuk MG, Izrael YA, Janssens A, Jones AR, Kelly GN, Kvasnikova EV, Matveenko IL, Nazarov IM, Pokumeiko YuM, Sitak VA, Stukin ED, Tabachny LY, Tsaturov YS, Avdyushin SI (1998) Atlas of caesium deposition on Europe after the Chernobyl accident, EUR 16733 EC. Office for Official Publications of the European Communities, Luxembourg

DeJong E, Begg CBM, Kachanoski RG (1983) Estimates of soil-erosion and deposition for some Saskatchewan soils. Can J Soil Sci 63:607–617

DeJong E, Wang C, Rees HW (1986) Soil redistribution on three cultivated New Brunswick hillslopes calculated from ^{137}Cs measurement, solum data and the USLE. Can J Soil Sci 66:721–730

Department of National Health and Welfare (1986) Environmental radioactivity in Canada (Radiological monitoring annual report). Department of National Health and Welfare, Ottawa

Devereux OH, Prestegaard KL, Needleman BA, Gellis AC (2010) Suspended-sediment sources in an urban watershed, Northeast Branch Anacostia River, Maryland. Hydrol Process (www.interscience.wiley.com). doi:10.1002/hyp.7604

Diamond J (2005) Collapse: how societies choose to fail or succeed. Viking, New York

Dibb JE (1989) Atmospheric deposition of beryllium-7 in the Chesapeake Bay region. J Geophys Res 94:2261–2265

Dietrich WE, Dunne T (1978) Sediment budget for a small catchment in mountainous terrain. Z Geomorphol Suppl Bd 29:191–206

Doering C, Akber R, Heijnis H (2006) Vertical distributions of Pb-210 excess, Be-7 and Cs-137 in selected grass covered soils in Southeast Queensland, Australia. J Environ Radioact 87:135–147

Dong A, Chesters G, Simsiman GV (1984) Metal composition of soil, sediments, and urban dust and dirt samples form the Menomonee River watershed, Wisconsin, USA. Water Air Soil Pollut 22:257–275

Dorman L (2004) Cosmic rays in the Earth's atmosphere and underground. Kluwer Academic, Dordrecht

Dorr H, Munnich KO (1989) Downward movement of soil organic matter and its influence on trace-element transport (^{210}Pb, ^{137}Cs) in the soil. Radiocarbon 31:655–663

Durana L, Chudy M, Masarik J (1996) Investigations of Be-7 in the Brastislava atmosphere. J Radioanal Nucl Chem 207:345–356

Dutkiewicz VA, Husain L (1985) Stratospheric and tropospheric components of ^{7}Be in surface air. J Geophy Res 90:5783–5788

EC/IGCE (1998) Roshydromet (Russia)/Minchernobyl (Ukraine)/Belhydromet (Belarus)

El-Hussein A, Mohamemed A, Abd El-Hady M, Ahmed AA, Ali AE, Barakat A (2001) Diurnal and seasonal variation of short-lived radon progeny concentration and atmospheric temporal variations of Pb-210 and Be-7 in Egypt. Atmos Environ 35:4305–4313

Environmental Protection Agency (2000) National water quality inventory, 2000 report. URL:http://www.epa.gov/305b/2000report/. Accessed date: March 19, 2010

Février L, Martin-Garin A (2005) Biogeochemical behaviour of anionic radionuclides in soil: evidence for biotic interactions. Radioprotection 40:S79–S86

Fisher GB, Magilligan FJ, Kaste JM, Nislow KH (2010) Constraining the timescales of sediment sequestration with large woody debris using cosmogenic ^{7}Be. J Geophys Res 115: doi:10.129/2009JF001352

Fitzgerald SA, Klump JV, Swarzenski PW, Mackenzie RA, Richards KD (2001) Beryllium-7 as a tracer of short-term sediment deposition and resuspension in the Fox River, Wisconsin. Environ Sci Technol 35:300–305

Flavin C (1987) Reassessing nuclear power: the fallout from Chernobyl. Worldwatch paper 75, Washington

Flury MS, Czigany S, Chen G, Harsh JB (2004) Cesium migration in saturated silica sand and Hanford sediments as impacted by ionic strength. J Contam Hydrol 71:111–126

Fondran CL (2007) Characterizing erosion by laser scanning. M.A. Thesis, Case Western Reserve University, 60 pp

Fornes WL, Matisoff G, Wilson CG, Whiting PJ (2000) Cs-137-derived soil erosion rates under changing tillage practices. EOS Transactions, Amer. Geophys. Union Fall Meeting, San Francisco, CA

Fornes WL, Matisoff G, Wilson CG, Whiting PJ (2005) Erosion rates using Cs-137; the effects of model assumptions and management practices. Earth Surf Process Landforms 30:1181–1189

Foster IDL, Dalgleish H, Deargin JA, Jones ED (1994) Quantifying soil erosion and sediment transport in drainage basins; some observations on the use of ^{137}Cs. In: Variability in stream erosion and sediment transport. IAHS Press, Wallingford

Gabet EJ (2000) Gopher bioturbation: field evidence for non-linear hillslope diffusion. Earth Surf Process Landforms 25:1419–1428

Gabet EJ, Reichman OJ, Seabloom EW (2003) The effects of bioturbation on soil processes and sediment transport. Ann Rev Earth Planet Sci 31:249–273

Gallagher D, McGee EJ, Mitchell PI (2001) A recent history of C-14, Cs-137 and Pb-210 accumulation in Irish peat bogs: an east versus west coast comparison. In: RadioCarbon conference, Jerusalem, June 2000

Gellis AC, Landwehr JM (2006) Identifying sources of fine-grained suspended-sediment for the Pocomoke River, an Eastern Shore tributary to the Chesapeake Bay. In: Proceedings of the 8th federal interagency sedimentation conference, Reno, Nevada, 2–6 April 2006, Reno, NV, Paper 5C-1 in CD_ROM file ISBN 0-9779007-1-1, 9

Goldberg ED, Koide M (1962) Geochronological studies of deep sea sediments by the ionium/thorium method. Goeochim Cosmochim Acta 26:417–450

Goodbred SL, Kuehl SA (1998) Floodplain processes in the Bengal Basin and the storage of Ganges-Brahmaputra river sediment: an accretion study using ^{137}Cs and ^{210}Pb geochronology. Sediment Geol 121:239–258

Govers G, Vandaele K, Desmet P, Poesen J, Bunte K (1994) The role of tillage in soil redistribution on hillslopes. Eur J Soil Sci 45:469–478

Govers G, Quine TA, Desmet PJ, Walling DE (1996) The relative contribution of soil tillage and overland flow erosion to soil redistribution on agricultural land. Earth Surf Process Landforms 21:929–946

Harden JW, Sundquist ET, Stallard RF, Mark RK (1992) Dynamics of soil carbon during deglaciation of the Laurentide ice sheet. Science 258:1921–1924

Hawley N, Robbins JA, Eadie BJ (1986) The partitioning of ^{7}beryllium in fresh water. Geochim Cosmochim Acta 50:1127–1131

He Q, Owens P (1995) Determination of suspended sediment provenance using caesium-137, unsupported lead-210 and radium-226; a numerical mixing model approach. In: Gurnell A, Webb B, Foster I (eds) Sediment and water quality in river catchments. London, Wiley, pp 207–227

He Q, Walling DE (1996) Interpreting particle size effects in the adsorption of ^{137}Cs and unsupported ^{210}Pb by mineral soils and sediments. J Environ Radioact 30:117–137

Health and Safety Laboratory (1977) Final tabulation of monthly ^{90}Sr fallout data: 1954–1976. USERDA Report HASL-329

Heckrath G, Halekoh U, Djurhuus J, Govers G (2006) The effect of tillage direction on soil redistribution by mouldboard ploughing on complex slopes. Soil Tillage Res 88:225–241

Hicks HG (1982) Calculation of the concentration of any radionuclide deposited on the ground by off-site fallout from a nuclear detonation. Health Phys 42:585–600

Honeyman BD, Ranville JF (2002) Colloid properties and their effects on radionuclide transport through soils and groundwater. In: Zhang P-C, Brady PV (eds.) Geochemistry of soil radionuclides. SSSA special publication 59; Soil Science Society of America, Madison, pp 131–163

Hong G-H, Hamilton TF, Baskaran M, Kenna TC (2011) Applications of anthropogenic radionuclides as tracers to investigate marine environmental processes. In: Baskaran M (ed) Handbook of environmental isotope geochemistry. Springer, Heidelberg

Hu Y, Liu J, Zhuang D, Cao H, Yan H, Yang F (2005) Distribution characteristics of ^{137}Cs in wind-eroded soil profile and its use in estimating wind erosion modulus. Chin Sci Bull 50:1155–1159

Hyams E (1952) Soil and civilization. Thames and Hudson, London

Ioannidou A, Papastefanou C (2006) Precipitation scavenging of Be-7 and Cs-137 radionuclides in air. J Environ Radioact 85:121–136

Jarvis NJ, Taylor A, Larsbo M (2010) Modeling the effects of bioturbation on the re-distribution of ^{137}Cs in an undisturbed grassland soil. Eur J Soil Sci 61:24–34

Johnson DL, Keller EA, Rockwell TK (1990) Dynamic pedogenesis – new views on some key soil concepts, and a model for interpreting quaternary soils. Quat Res 33:306–319

Joshi SR (1987) Early Canadian results on the long-range transport of chernobyl radioactivity. Sci Total Environ 63:125–137

Jweda J, Baskaran M, van Hees E, Schweitzer L (2008) Short-lived radionuclides (Be-7 and Pb-210) as tracers of particle dynamics in a river system in southeast Michigan. Limnol Oceanogr 53:1934–1944

Kachanoski RG, deJong E (1984) Predicting the temporal relationship between soil cesium-137 and erosion rate. J Environ Qual 13:301–304

Kaste JM, Baskaran M (2011) Meteoric ^{7}Be and ^{10}Be as process tracers in the environment. In: Baskaran M (ed) Handbook of environmental isotope geochemistry. Springer, Heidelberg

Kaste JM, Fernandez IJ, Hess CT, Norton SA, Pillerin BA (1999a) Sinks and mobilization of cosmogenic beryllium-7 and bedrock-derived beryllium-9 in forested watersheds in Maine, USA. Geol Soc Am Abst Prog 31:305

Kaste JM, Fernandez IJ, Hess CT, Norton SA (1999b) Delivery of cosmogenic beryllium-7 to forested watersheds in Maine, USA. Geol Soc Am Abst Progr 31:305

Kaste JM, Norton SA, Hess CT (2002) Environmental chemistry of beryllium-7. Rev Mineral Geochem 50:271–289

Kaste JM, Heimsath AM, Hohmann M (2006) Quantifying sediment transport across an undisturbed prairie landscape using cesium-137 and high resolution topography. Geomorphology 76:430–440

Kaste JM, Heimseth AM, Bostick BC (2007) Short-term soil mixing quantified with fallout radionuclides. Geology 35:243–246

Ketterer ME, Szechenyi SC (2008) Determination of plutonium and other transuranic elements by inductively coupled plasma mass spectrometry: a historical perspective and new frontier in the environmental sciences. Spectrochim Acta 63:719–737

Ketterer ME, Watson BR, Matisoff G, Wilson CG (2002) Rapid dating of recent aquatic sediments using Pu activities and ^{240}Pu/^{239}Pu as determined by quadrupole inductively coupled plasma mass spectrometry. Environ Sci Technnol 36:1307–1311

Ketterer ME, Hafer KM, Mietelski JW (2004) Resolving Chernobyl vs. global fallout contributions in soils from Poland using plutonium atom ratios measured by inductively coupled plasma mass spectrometry. J Environ Radioact 73:183–201

Ketterer ME, Zheng J, Yamada M (2011) Source tracking of transuranics using their isotopes. In: Baskaran M (ed) Handbook of environmental isotope geochemistry. Springer, Heidelberg

Kikuchi S, Sakurai H, Gunji S, Tokanai F (2009) Temporal variation of Be-7 concentrations in atmosphere for 8 y

from 2000 at Yamagata, Japan: solar influence on the Be-7 time series. J Environ Radioact 100:515–521

Koch DM, Jacob DJ, Graustein WC (1996) Vertical transport of tropospheric aerosols as indicated by ^{7}Be and ^{210}Pb in a chemical tracer model. J Geophys Res 101:18651–18666

Konshin OV (1992) Mathematical model of ^{137}Cs migration in soil: analysis of observations following the Chernobyl accident. Health Phys 63:301–306

Korky JK, Kowalski L (1989) Radioactive cesium in edible mushrooms. J Agric Food Chem 37:568–569

Korobova E, Ermakov A, Linnak V (1998) ^{137}Cs and ^{90}Sr mobility in soils and transfer in soil-plant systems in the Novozybkov district affected by the Chernobyl accident. Appl Geochem 13:803–814

Kownacka L (2002) Vertical distributions of beryllium-7 and lead-210 in the tropospheric and lower stratospheric air. Nukleonika 47:79–82

Lal D, Baskaran M (2011) Applications of cosmogenic-isotopes as atmospheric tracers. In: Baskaran M (ed) Handbook of environmental isotope geochemistry. Springer, Heidelberg

Lal D, Peters B (1967) Cosmic ray produced radioactivity on the Earth, p. 551–612. In Encyclopedia of physics. V. 46/2. Springer

Lal R (2003) Soil erosion and the global carbon budget. Environ Internat 29:437–450

Lance J, McIntyre SC, Naney JW, Rousseva SS (1986) Measuring sediment movement at low erosion rates using cesium 137. Soil Sci Soc Am J 50:1303–1309

Lenhart JJ, Saiers JE (2002) Transport of silica colloids through unsaturated porous media: experimental results and model comparisons. Environ Sci Technol 36:769–777

Li M, Li ZB, Liu PL, Yao WY (2005) Using Cesium-137 technique to study the characteristics of different aspect of soil erosion in the wind-water erosion crisscross region on Loess Plateau of China. Appl Radiat Isot 62:109–113

Lobb DA, Kachanoski RG (1999) Modeling tillage translocation using step, linear-plateau and exponential functions. Soil Till Res 51:317–330

Lobb DA, Kachanoski RG, Miller MH (1995) Tillage translocation and tillage erosion on shoulder slope landscape positions measured using Cs-137 as a tracer. Can J Soil Sci 75:211–218

Lobb DA, Kachanoski RG, Miller MH (1999) Tillage translocation and tillage erosion in the complex upland landscapes of southwestern Ontario, Canada. Soil Tillage Res 51:189–209

Lomenick TF, Tamura T (1965) Naturally occurring fixation of cesium-137 on sediments of lacustrian origin. Soil Sci Soc Am Proc 29:383–386

Loughran J, Elliott GL, Campbell BL, Shelly DJ (1988) Estimation of soil erosion from caesium-137 measurements in a small, cultivated catchment in Australia, Applied Radiation and Isotopes A39, pp. 1153–1157

Lowdermilk WC (1953) Conquest of the land through 7000 years. Agricultural Info Bull No. 99

Lowrance R, McIntyre S, Lance C (1988) Erosion and deposition in a field/forest system estimated using cesium-137 activity. J Soil Water Conserv 43:195–199

Lyles L (1985) Predicting and controlling wind erosion. Agric Hist Soc 59:205–214

Mabit L, Benmansour M, Walling DE (2008) Comparative advantages and limitations of the fallout radionuclides Cs-137, Pb-210(ex) and Be-7 for assessing soil erosion and sedimentation. J Environ Radioact 99:1799–1807

Martz LW, de Jong E (1985) The relationship between land surface morphology and soil erosion-deposition rates in a small Saskatchewan basin. Proceedings of the Canadian Society for Civil Engineering, Annual Conference, Hydrotechnical Division, July 1985, Saskatoon, Sask., 1–19

Matisoff G, Bonniwell EC, Whiting PJ (2002a) Soil erosion and sediment sources in an Ohio watershed using Beryllium-7, Cesium-137, and Lead-210. J Environ Qual 31:54–61

Matisoff G, Bonniwell EC, Whiting PJ (2002b) Radionuclides as indicators of sediment transport in agricultural watersheds that drain to Lake Erie. J Environ Qual 31:62–72

Matisoff G, Wilson GC, Whiting PJ (2005) ^{7}Be/^{210}Pb ratio as an indicator of suspended sediment age or fraction new sediment in suspension. Earth Surf Process Landforms 30:1191–1201

Matisoff G, Ketterer ME, Rosén K, Mietelski JW, Vitko LF, Persson H, Lokas E (2011) Downward Migration of Chernobyl-derived Radionuclides in Soils in Poland and Sweden. Applied Geochemistry 26:105–115

McHenry JR, Ritchie JC, Gill AC (1973) Accumulation of fallout cesium 137 in soils and sediments in selected watersheds. Water Resour Res 9:676–686

McNeary D, Baskaran M (2003) Depositional characteristics of Be-7 and Pb-210 in southeastern Michigan. J Geophys Res Atmos 108:4210

Mietelski JW, Was B (1995) Plutonium from Chernobyl in Poland. Appl Radiat Isot 46:1203–1211

Mietelski JW, Jasińska M, Kozak K, Ochab E (1996) The method of measurements used in the investigation of radioactive contamination of forests in Poland. Appl Radiat Isot 47:1089–1095

Miller KM, Kuiper JL, Helfer IK (1990) ^{137}Cs fallout depth distributions in forest versus field sites: implications for external gamma dose rates. J Environ Radioact 12:23–47

Montgomery DR (2007) Dirt: the erosion of civilizations. University of California Press, California

Montgomery JA, Busacca AJ, Frazier BE, McCool DK (1997) Evaluating soil movement using cesium-137 and the revised universal soil loss equation. Soil Sci Soc Am J 61:571–579

Motha JA, Walbrink PJ, Hairsine PB, Grayson RB (2002) Tracer properties of eroded sediment and source material. Hydrol Process 16:1983–2000

Müller-Lemans H, van Dorp F (1996) Bioturbation as a mechanism for radionuclide transport in soils: relevance of earthworms. J Environ Radioact 31:7–20

Nagle GN, Fahey T, Ritchie JC, Woodbury PB (2007) Variations in sediment sources in the Finger Lakes and Western Catskills regions of New York. Hydrol Process 21:828–838

Nelson DW, Logan TJ (1983) Chemical processes and transport of phosphorus. In: Schaller FW, Bailey GW (eds) Agricultural management and water quality. Iowa State University Press, Iowa

O'Farrell CR, Heimsath AM, Kaste JM (2007) Quantifying hillslope erosion rates and processes for a coastal California landscape over varying timescales. Earth Surf Process Landforms 32:544–560

Oldeman LR (1994) The global extent of soil degradation. In: Greland DJ, Szacolcs I (eds) Soil resilience and sustainable land use. CAB International, Wallingford, pp 99–118

Olsen CR, Larsen IL, Lowry PD, Cutshall NH, Todd JF, Wong GTF, Casey WH (1985) Atmospheric fluxes and marsh-soil inventories of ^{7}Be and ^{210}Pb. J Geophys Res 90:10487–10495

Olsen CR, Larsen IL, Lowry PD, Cutshall NH (1986) Atmospheric fluxes and marsh-soil inventories of ^{7}Be and ^{210}Pb. J Geophys Res 90:10487–10495

Owens PN, Walling DE (1996) Spatial variability of caesium-137 inventories at reference sites: an example from two contrasting sites in England and Zimbabwe. Appl Radiat Isot 47:699–707

Owens PN, Walling DE, He Q (1996) The behavior of bomb-derived caesium-137 fallout in catchment soils. J Environ Radioact 32:169–191

Owens PN, Walling DE, He Q, Shanahan J, Foster I (1997) The use of caesium-137 measurements to establish a sediment budget for the Start catchment, Devon, UK. Hydrol Sci 42:405–423

Paasikallio A (1999) Effect of biotite, zeolite, heavy clay, bentonite and apatite on the uptake of radiocesium by grass from peat soil. Plant Soil 206:213–222

Paatero J, Hatakka J (2000) Source areas of airborne Be-7 and Pb-210 measured in Northern Finland. Health Phys 79:691–696

Papastefanou C, Ioannidou A (1991) Depositional fluxes and other physical characteristics of atmospheric Beryllium-7 in the temperate zones (40N) with a dry (precipitation free) climate. Atmos Environ 25:2335–2343

Papastefanou C, Ioannidou A, Stoulos S, Manolopoulou M (1995) Atmospheric deposition of cosmogenic ^{7}Be and ^{137}Cs from fallout of the Chernobyl accident. Sci Total Environ 170:151–156

Pimental D, Harvey C, Resosuarmo P, Sinclair K, Kurz D, McNair M, Crist S, Shpritz L, Fitton L, Saffourni R, Blair R (1995) Environmental and economic costs of soil erosion and conservation benefits. Science 267:1117–1123

Porcelli D, Baskaran M (2011) An overview of isotope geochemistry in environmental studies. In: Baskaran M (ed) Handbook of environmental isotope geochemistry. Springer, Heidelberg

Poreba GJ (2006) Caesium-137 as a soil erosion tracer: a review. Geochronometria 25:37–46

Pote DH, Daniel TC, Sharpley AN, Moore PA, Edwards DR, Nichols DJ (1996) Relating extractable soil phosphorus to phosphorus losses in runoff. Soil Sci Soc Am J 60:855–859

Powell EN (1977) Particle size selection and sediment reworking in a funnel feeder, *Leptosynapta benvis* (Holothuroidea, Synaptidae). Int Rev Gesamten Hydrobiol 62:385–408

Provansal M, Villiet J, Eyrolle F, Raccasi G, Gurriaran R, Antonelli C (2010) High-resolution evaluation of recent bank accretion rate of the managed Rhone: a case study by multi-proxy approach. Geomorphology 117:287–297

Quine TA (1995) Estimation of erosion rates from Caesium-137 data; the calibration question. In: Foster IDL et al (eds) Sediment and water quality in river catchments. Chichester, Wiley, pp 307–329

Quine TA (1999) Use of caesium-137 data for validation of spatially distributed erosion models: the implications of tillage erosion. Catena 37:415–430

Quine TA, Zhang Y (2004) Re-defining tillage erosion: quantifying intensity – direction relationships for complex terrain. (1) Derivation of an adirectional soil transport coefficient. Soil Use and Management 20(2):114–123

Rabalais NN, Turner RE, Dubravko J, Dortsch Q, Wisman WJ (1999) Characterization of hypoxia: topic 1 report for the integrated assessment on hypoxia in the Gulf of Mexico. NOAA Coastal Ocean Program Decision Analysis Series No. 17, NOAA Coastal Ocean Office, Silver Spring

Reiser DW (1998) Sediment in gravel bed rivers. In: Klingeman PC, Beschta RL, Komar PD, Bradley JB (eds) Ecological and biological considerations. Water Resource Publications, Highland Ranch

Revelle P, Revelle C (1988) The environment. Jones and Bartlett, Boston

Rhoads DC (1974) Organism-sediment relations on the muddy sea floor. Oceanogr Mar Biol Annu Rev 12:263–300

Rhoads DC, Stanley DJ (1964) Biogenic graded bedding. J Sediment Petrol 35:956–963

Riise G, Bjornstad HE, Lien HN, Oughton DH, Saibu B (1990) A study on radionuclide association with soil components using a sequential extraction procedure. J Radioanal Nucl Chem 142:531–538

Ritchie JC, McHenry JR (1978) Fallout Cs-137 in cultivated and noncultivated North Central United States watersheds. J Environ Qual 7:40–44

Ritchie JC, McHenry JR (1990) Application of radioactive fallout Cesium-137 for measuring soil erosion and sediment accumulation rates and patterns – a review. J Environ Qual 19:215–233

Ritchie JC, Ritchie CA (2008) Bibliography of publications of ^{137}cesium studies related to erosion and sediment deposition. http://web.cena.usp.br/apostilas/Osny/BiblioCs137December2008.pdf. Accessed 21 Jan 2010

Ritchie JC, Spraberry JA, McHenry JR (1974) Estimating soil erosion for the redistribution of fallout ^{137}Cs. Soil Sci Soc Am J 38:137–139

Robbins JA (1985) Great Lakes regional fallout source functions. NOAA Technical Memorandum ERL GLERL-56, Ann Arbor, MI

Robbins JA (1986) A model for particle-selective transport of tracers in sediments with conveyor-belt deposit feeders. J Geophys Res 91(C7):8542–8558

Robbins JA, Eadie BJ (1991) Seasonal cycling of trace elements ^{137}Cs, ^{7}Be, and $^{239+240}$Pu in Lake Michigan. J Geophy Res 96:17081–17104

Robbins JA, McCall PL, Fisher JB, Krezoski JR (1979) Effect of deposit feeders on migration of ^{137}Cs in lake sediment. Earth Planet Lett 42:277–287

Rogowski AS, Tamura T (1970) Environmental mobility of cesium-137. Radiat Bot 10:35–45

Rosen K, Oborn L, Lonsjo H (1999) Migration of radiocaesium in Swedish soil profiles after the Chernobyl accident, 1987–1995. J Environ Radioact 46:45–66

Rowan JS (1995) The erosional transport of radiocaesium in catchment systems: a case study of the Exe basin, Devon. In: Foster IDL et al (eds) Sediment and water quality in river catchments. Wiley, Chichester

Roy JC, Cote JE, Mahfoud A, Villeneuve S, Turcotte J (1988) On the transport of Chernobyl radioactivity to eastern Canada. J Environ Radioact 6:121–130

Salant NL, Renshaw CE, Magilligan FJ, Kaste JM, Nislow KH, Heimsath AM (2006) The use of short-lived radionuclides to quantify transitional bed material transport in a regulated river. Earth Surf Process Landforms 32:509–524

Salisbury RT, Cartwright J (2005) Cosmogenic Be-7 deposition in North Wales: Be-7 concentrations in sheep faeces in relation to altitude and precipitation. J Environ Radioact 78:353–361

Sanchez AL, Wright SM, Smolders E, Naylor C, Stevens PA, Kennedy VH, Dodd BA, Singleton DL, Barnett CL (1999) High plant uptake of radiocesium from organic soils due to Cs mobility and low soil K content. Environ Sci Technol 33:2752–2757

Sarmiento JL, Gwinn E (1986) Strontium-90 fallout prediction. J Geophys Res 91:7631–7646

Schuller P, Elliers A, Kirchner G (1997) Vertical migration of fallout ^{137}Cs in agricultural soils from Southern Chile. Sci Total Environ 193:197–205

Schuller P, Iroume A, Walling DE, Mancilla HB, Castillo A, Trumper RE (2006) Use of beryllium-7 to document soil redistribution following forest harvest operations. J Environ Qual 35:1756–1763

Schultz RK, Overstreet R, Barshad I (1959) On the soil chemistry of cesium-137. Soil Sci 89:19–27

Sekely AC, Bauer DW, Mulla DJ (2002) Streambank slumping and its contribution to the phosphorus and suspended sediment loads of the Blue Earth River, Minnesota. J Soil Water Conserv 57:243–250

Sepulveda A, Schuller P, Walling DE, Castillo A (2008) Use of Be-7 to document soil erosion associated with a short period of extreme rainfall. J Environ Radioact 99:35–49

Sharpley AN, Daniel TC, Edwards DR (1994) Phosphorus movement in the landscape. J Product Agric 6:492–500

Shenber MA, Johanson KJ (1992) Influence of zeolite on the availability of radiocaesium in soil to plants. Sci Total Environ 113:287–295

Shimmack W, Flessa H, Bunzl K (1997) Vertical migration of Chernobyl-derived radiocesium in Bavarian Grassland soils. Naturvissenschaften 84:204–207

Siggars GB, Bates PD, Anderson MG, Walling DE, He Q (1999) A preliminary investigation of the integration of modeled floodplain hydraulics with estimates of overbank floodplain sedimentation derived form Pb-210 and Cs-137 measurements. Earth Surf Process Landforms 24: 211–231

Soileau JM, Hajek BF, Touchton JT (1990) Soil erosion and deposition evidence in a small watershed using fallout cesium-137. Soil Sci Soc Am J 54:1712–1719

Spomer RG, McHenry JR, Piest RF (1985) Sediment movement and deposition using cesium-137 tracer. Trans Am Soc Agric Eng 28:767–772

St Gerontidis DV, Kosmas G, Detsis G, Marathianou M, Zafirios T, Tsara M (2001) The effect of mouldboard plow on tillage erosion along a hillslope. J Soil Water Conserv 56:147–152

Stallard RF (1998) Terrestrial sedimentation and the carbon cycle: coupling weathering and erosion to carbon burial. Global Biogeochem Cy 12:231–257

Steinmann P, Billen T, Loizeau J-L, Dominik J (1999) Beryllium-7 as a tracer to study mechanisms and rates of metal scavenging from lake surface waters. Geochim Cosmochim Acta 63:1621–1633

Stokes S, Walling DE (2003) Radiogenic and isotopic methods for the direct dating of fluvial sediments. In: Kondolf GM, Piegay H (eds) Tools in fluvial geomorphology. Wiley, Chichester

Stubblefield AP, Fondran C, Ketterer ME, Matisoff G, Whiting PJ (2006) Radionuclide and rare earth element tracers of erosional processes on the plot scale. In: Joint Eighth Federal Interagency Sedimentation Conference and Third Federal Interagency Modeling Conference, Reno, Nevada

Stubblefield AP, Whiting PJ, Matisoff G, Fondran C, Wilson C, Calhoun FC, ms. Delivery of nutrients by rill and sheet erosion in agricultural settings. In preparation

Su CC, Huh CA, Lin FJ (2003) Factors controlling atmospheric fluxes of Be-7 and Pb-210 in northern Taiwan. Geophys Res Lett 30:2018

Sugihara S, Momoshima N, Maeda Y, Osaki S (2000) Variation of atmospheric ^{7}Be and ^{210}Pb depositions at Fukuoka, Japan. In: 10th international congress of the international radiation protection association. Hiroshima, Japan 10–19 May 2000

Sutherland RA, deJong E (1990) Estimation of sediment redistribution within agricultural fields using caesium-137. Crystal Springs, Saskatchewan, Canada. Appl Geograph 10:205–213

Sutherland RA, Kowalchuk T, deJong E (1991) Caesium-137 estimates of sediment redistribution by wind. Soil Sci 151:387–396

Tamura T, Jacobs DG (1960) Structural implications in cesium sorption. Health Phys 2:391–398

Tarras-Wahlberg NH, Lane SN (2003) Suspended sediment yield and metal contamination in a river catchment affected by El Nino events and gold mining activities; the Puyango River Basin, Southern Ecuador. Hydrol Process 17:3101–3123

Todd JF, Wong GRF, Olsen CR, Larsen IL (1989) Atmospheric depositional characteristics of Beryllium 7 and Lead 210 along the southeastern Virginia Coast. J Geophys Res 94:11106–11116

Tokieda T, Yamanaka K, Harada K, Tsunogai S (1996) Seasonal variation of residence time and upper atmospheric contribution of aerosols studied with Pb-210, Po-210 and Be-7. Tellus 48:690–702

Turekian KK, Nozaki Y, Benninger LK (1977) Geochemistry of atmospheric radon and radon products. Ann Rev Earth Planet Sci 5:227–255

Turekian KK, Benninger LK, Dion EP (1983) ^{7}Be and ^{210}Pb total deposition fluxes at New Haven, Connecticut and at Bermuda. J Geophys Res 88:5411–5415

Valles I, Camacho A, Ortega X (2009) Natural and anthropogenic radionuclides in airborne particulate samples collected in Barcelona (Spain). J Environ Radioact 100:102–107

Van Muysen W, Govers G, Van Oost K (2002) Identification of important factors in the process of tillage erosion: the case of mouldboard tillage. Soil Till Res 65:77–93

Van Oost K, Govers G, de Albe S, Quine TA (2006) Tillage erosion: a review of controlling factors and implications for soil quality. Progr Phys Geog 4:443–466

Vitko L (2007) Evaluating soil erosion on agricultural plots using radionuclides. BA Thesis, Case Western Reserve University

Wallbrink PJ, Murray AS (1994) Fallout of ^{7}Be in south Eastern Australia. J Environ Radioact 25:213–228

Wallbrink PJ, Murray AS (1996) Distribution and variability of Be-7 in soils under different surface cover conditions and its potential for describing soil redistribution processes. Water Resour Res 32:467–476

Wallbrink PJ, Murray AS, Olley JM (1999) Relating suspended sediment to its original soil depth using fallout radionuclides. Soil Science Society of America Journal 63:369–378

Walling DE, He Q (1997a) Investigating spatial patterns of overbank sedimentation on river floodplains. Water Air Soil Pollut 99:9–20

Walling DE, He Q (1997b) Models for converting ^{137}Cs measurements to estimates for soil redistribution on cultivated and uncultivated soils (including software for model implementation). In: International Atomic Energy Agency (IAEA) coordinated research programmes on soil erosion (D1.50.05) and sedimentation (F3.10.01). University of Exeter, Exeter

Walling DE, Quine TA (1990) Calibration of cesium-137 measurements to provide quantitative erosion rate data. Land Degrad Rehab 2:161–175

Walling DE, Quine TA (1992) The use of caesium-137 measurements in soil erosion surveys. In: Erosion and sediment transport monitoring programmes in River Basins, IAHS publications 210, Wallingford

Walling DE, Quine TA (1993) Use of caesium-137 as a tracer of erosion and sedimentation: Handbook for the application of the caesium-137 technique. U.K Overseas Development Administration Research Scheme R4579, Department of Geography, University of Exeter, Exeter, United Kingdom, 196 p

Walling DE, Woodward JC (1992) Use of radiometric fingerprints to derive information on suspended sediment sources. In: Erosion and sediment transport monitoring programmes in River Basins, IAHS publications 210, Wallingford

Walling DE, He Q, Blake W (1999a) Use of Be-7 and Cs-137 measurements to document short- and medium term rates of water-induced soil erosion on agricultural land. Water Resour Res 35:3865–3874

Walling DE, Owens PN, Leeks GJL (1999b) Fingerprinting suspended sediment sources in the catchment of the River Ouse, Yorkshire, UK. Hydrol Process 13:955–975

Walling DE, He Q, Appleby PG (2002) Conversion models for use in soil-erosion, soil-redistribution and sedimentation investigations. In: Zapata F (ed) Handbook for the assessment of soil erosion and sedimentation using environmental radionuclides. Kluwer Academic Publishers, Dordrecht, pp 111–164

Walling DE, Collins AL, Sichingabula HM (2003) Using unsupported lead-210 measurements to investigate erosion and sediment delivery in a small Zambian catchment. Geomorphology 52:193–213

Walling DE, Schuller P, Zhang Y, Iroume A (2009) Extending the timescale for using beryllium 7 measurements to document soil redistribution by erosion. Water Resour Res 45: W02418

Wang K, Cornett RJ (1993) Distribution coefficients of ^{210}Pb and ^{210}Po in laboratory and natural aquatic systems. J Paleolimnol 9:179–188

Whiting PJ, Bonniwell EC, Matisoff G (1999) A Mass Balance Method for Determining the Depth and Area of Rill and Sheetwash Erosion of Soils using Fallout Radionuclides (^{7}Be, ^{137}Cs, ^{210}Pb): EOS Transactions, American Geophysical Union Fall Meeting. v. 80. p. F445

Whiting PJ, Bonniwell EC, Matisoff G (2001) Depth and areal extent of sheet wash and rill erosion from radionuclides in soils and suspended sediment. Geology 29:1131–1134

Whiting PJ, Matisoff G, Fornes W, Soster F (2005) Suspended sediment sources and transport distances in the Yellowstone basin. Geol Soc Am Bull 117:515–529

Williams GP, Wolman MG (1984) Downstream effects of dams on alluvial rivers. US Geological Survey Professional Paper 1286, p 83

Wilson CG, Matisoff G, Whiting PJ (2003) Short-term erosion rates from a Be-7 inventory balance. Earth Surf Process Landforms 28:967–977

Wilson CG, Matisoff G, Whiting PJ (2005) Transport of fine sediment through the Old Woman Creek, OH, wetland using radionuclide tracers. J Great Lakes Res 31:56–67

Wilson CG, Matisoff G, Whiting PJ (2007) The use of ^{7}Be and $^{210}Pb_{xs}$ to differentiate suspended sediment sources in South Slough, OR. Estuar Coasts 30:348–358

Wischmeier WH, Smith DD (1978) Predicting rainfall erosion losses – a guide to conservation planning. In: Agricultural handbook No. 537. US Department of Agricultural Science and Education Administration, Washington

Wise SW (1980) Caesium-137 and lead-210: a review of the technique and application to geomorphology, pp. 109–127. In: Cullingford RA, Davidson RA, Lewin J (eds) Timescales in geomorphology, John Wiley and Sons, New York

Yamada H, Nakamura F (2002) Effect of fine sediment deposition and channel works on periphyton biomass in the Makomanai River, Northern Japan. River Res Appl 18:481–493

Yan P, Shi P (2004) Using the ^{137}Cs technique to estimate wind erosion in Gonghe Basin, Qinghai Province, China. China Soil Sci 169:295–305

Yan P, Zhang XB (1998) Prospects of caesium-137 used in the study of aeolian processes. J Desert Res 18:182–187

Yan P, Dong Z, Dong G, Zhang X, Zhang Y (2001) Preliminary results of using ^{137}Cs to study wind erosion in the Qinghai-Tibet plateau. J Arid Environ 47:443–452

You CF, Lee T, Li YH (1989) The partition of Be between soil and water. Chem Geol 77:105–118

Zapata F, Garcia-Agudo E, Ritchie JC, Appleby PG (2002) Introduction. In: Zapata F (ed) Handbook for the assessment of soil erosion and sedimentation using environmental radionuclides. Kluwer Academic Publishers, Dordrecht, pp 1–14

Zhang XB, Higgitt DL, Walling DE (1990) A preliminary assessment of the potential for using cesium-137 to estimate rates of soil-erosion in the Loess Plateau of China. Hydrol Sci 35:243–252

Zhang XB, Walling DE, He Q (1999) Simplified mass balance models for assessing soil erosion rates and cultivated land using cesium-137 measurements. Hydrol Sci 44:33–45